



ELSEVIER

Nuclear Physics B 645 (2002) 105–133



www.elsevier.com/locate/npe

Multi-caloron solutions

Falk Bruckmann, Pierre van Baal

*Instituut-Lorentz for Theoretical Physics, University of Leiden, PO Box 9506,
NL-2300 RA Leiden, The Netherlands*

Received 4 September 2002; accepted 17 September 2002

Abstract

We discuss the construction of multi-caloron solutions with non-trivial holonomy, both as approximate superpositions and exact self-dual solutions. The charge k $SU(n)$ moduli space can be described by kn constituent monopoles. Exact solutions help us to understand how these constituents can be seen as independent objects, which seems not possible with the approximate superposition. An “impurity scattering” calculation provides relatively simple expressions. Like at zero temperature an explicit parametrization requires solving a quadratic ADHM constraint, achieved here for a class of axially symmetric solutions. We will discuss the properties of these exact solutions in detail, but also demonstrate that interesting results can be obtained without explicitly solving for the constraint. © 2002 Elsevier Science B.V. All rights reserved.

PACS: -10.10.Wx; 12.38.Lg; 14.80.Hv

1. Introduction

The last four years more understanding has been gained of the interplay between instantons and monopoles in non-Abelian gauge theories, based on the ability to construct exact caloron solutions, i.e., instantons at finite temperature for which A_0 approaches a constant at spatial infinity [1,2]. This last condition is best expressed by specifying the Polyakov loop to approach a constant value at infinity, also called the holonomy. It is the finite action that demands the field strength to go to zero at infinity, and guarantees the Polyakov loop to be independent of the direction in which we approach infinity. One can parametrize this Polyakov loop in terms of its eigenvalues $\exp(2\pi i \mu_j)$ and a gauge rotation

E-mail address: vanbaal@lorentz.leidenuniv.nl (P. van Baal).

g , such that

$$\mathcal{P}_\infty = \lim_{x \rightarrow \infty} P \exp \left(\int_0^\beta A_0(\vec{x}, t) dt \right) = g^\dagger \exp(2\pi i \text{diag}(\mu_1, \mu_2, \dots, \mu_n)) g, \quad (1)$$

which can be arranged such that $\sum_{i=1}^n \mu_i = 0$, and $\mu_1 \leq \mu_2 \leq \dots \leq \mu_n \leq \mu_{n+1}$, with $\mu_{n+k} \equiv 1 + \mu_k$. This is in the gauge where the gauge fields, assumed to be anti-hermitian matrices taking values in the algebra of $SU(n)$, are periodic in the time direction $A_\mu(\vec{x}, t) = A_\mu(\vec{x}, t + \beta)$. In our conventions the field strength is given by $F_{\mu\nu}(x) = \partial_\mu A_\nu(x) - \partial_\nu A_\mu(x) + [A_\mu(x), A_\nu(x)]$.

We will find it convenient to construct the multi-caloron solutions from the ADHM–Nahm Fourier construction [1–4] based on taking instantons in R^4 , which periodically repeat in the time direction (see also Ref. [5] which uses directly the Nahm transformation [4, 6] as the starting point for the charge 1 construction). To allow for non-trivial holonomy, the periodicity is only up to a constant gauge rotation (which is the holonomy). In this so-called algebraic gauge, all gauge field components vanish at spatial infinity, and we may approximately superpose these calorons by simply adding the gauge fields. When each gauge field is periodic up to the same constant gauge transformation, the sum satisfies the same property. It should be noted that we are not allowed to add gauge fields with different holonomy; in an *infinite* volume the holonomy is fixed by the boundary condition. As to the topological charge, we recall that in the Atiyah–Drinfeld–Hitchin–Manin (ADHM) construction [3] it is supported by gauge singularities (the algebraic gauge is for this reason also called the singular gauge), as opposed to at infinity being a pure gauge with the gauge function having the appropriate winding number. To deal with the gauge singularity of one instanton, when adding the field of the others, one has to smoothly deform the gauge field of the latter to vanish near the gauge singularity. As long as the singularities are not too close, this can be done without a significant increase in the action. On the lattice this problem does not occur, when hiding singularities between the meshes of the lattice.

Calorons, however, have an additional feature. When squeezed in the imaginary time direction (the size ρ becoming bigger than the period β), they split in constituent monopoles with masses $8\pi^2 v_j / \beta$ ($v_j \equiv \mu_{j+1} - \mu_j$). Outside the cores of these monopoles the gauge field becomes abelian. Ignoring the charged components, which decay exponentially outside the cores of the constituent monopoles, the field is described in terms of self-dual Dirac monopoles. The singularity of a Dirac string can only be avoided by *not* neglecting the contributions coming from the charged components, even when far away from the constituents. For a single caloron we would not care, since the Dirac string is not seen in gauge invariant quantities. It does, however, involve a rather subtle interplay between the charged and neutral components of the gauge field in the vicinity of the would-be Dirac string [1]. It is this subtle interplay that is disturbed when we add gauge fields of various calorons together. Unlike for the gauge singularity, the combined field will not diverge, but it shows a narrow and steep enhancement at the location of the would-be Dirac string as illustrated in Fig. 1, where we added two $SU(2)$ calorons. Also here one may shield the Dirac strings from these tails. But one always pays the price that the Dirac string no longer can be hidden, and carries energy. Let us stress again that these are genuine

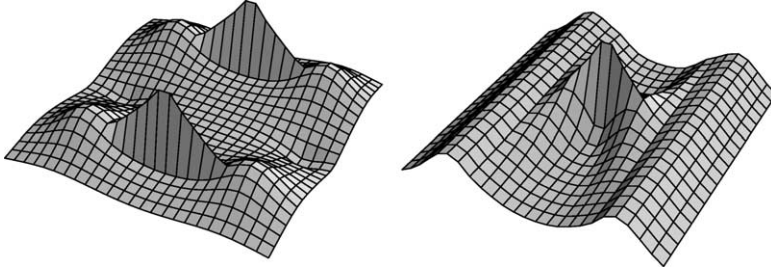


Fig. 1. Approximate superposition of two $SU(2)$ charge 1 calorons with its pairs of equal mass constituents at $\vec{x} = (2, 0, 2)$, $(2, 0, 8)$ and $\vec{x} = (8, 0, 2)$, $(8, 0, 8)$. The logarithm of the action density is plotted as a function of x and z . The plot on the right shows one of the would-be Dirac strings, zooming in by a factor 40 on the transverse direction.

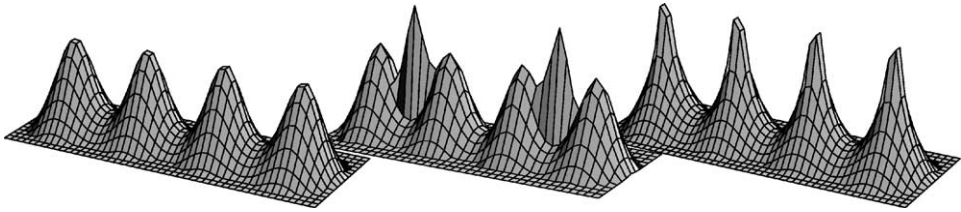


Fig. 2. Comparing the logarithm of the action density (cutoff for $\log(S)$ below -3 and above 7) as a function of x and z for the exact $SU(2)$ solution ($\mu_2 = \frac{1}{4}$) with charge 2 (left) with the approximate superposition of two charge one calorons (middle) and the Abelian solution based on Dirac monopoles (right), all on the same scale. The two pairs of constituent monopoles are located at $\vec{x} = (0, 0, 6.031)$, $(0, 0, 2.031)$ and $\vec{x} = (0, 0, -2.031)$, $(0, 0, -6.031)$.

gauge invariant non-singular features in the configuration, even though they are of course a consequence of our particular way of constructing a superposition.

A visible would-be Dirac string presents a formidable obstacle to considering the constituents as independent objects; they remember to which caloron they belong. Insisting the Abelian field far from the constituents to be exactly additive under the approximate superposition leaves us little room for considering other possible superpositions, apart from carefully fine-tuning the charged components of the configuration. Solving for the exact self-dual caloron solutions of higher charge we wish to show that a visible Dirac string is an artifact of the particular procedure to construct approximate caloron solutions. For the exact charge k caloron solutions we expect kn constituents and from the point of view of the parameter space these can be expected to be independent (as long the constituents do not get too close together).

In this paper we develop the formalism and give exact solutions for a class of axially symmetric solutions. For $SU(2)$ an example of such an exact solution with charge 2 is presented in Fig. 2. We compare the exact solution (left), with the one obtained by adding two charge 1 calorons, showing the would-be Dirac strings (middle) and with the exact Abelian solution determined from (self-dual) Dirac monopoles placed at the location of the constituents (right). Indeed, the would-be Dirac strings are no longer visible for the exact non-Abelian solution. This gives us good reasons to expect that moving away from the

requirement of axial symmetry, the exact solutions will exhibit the constituent monopoles as independent objects. This is an important prerequisite for attempting to formulate the long distance features of QCD in terms of these monopoles. Non-linearities will remain important when constituents overlap, like for instantons at zero-temperature, as will be illustrated through suitable examples.

Our results can also be used to extract information on multi-monopole solutions. In the charge 1 case it has been shown [1] that sending one of the constituents to infinity one is left with exact monopole solutions. Perhaps somewhat surprisingly, it has been notoriously difficult to construct approximate superpositions of magnetic monopoles in such a way the interaction energy decreases with their separation. Within our approach this is due to the difficulty (particularly when sending some constituents to infinity) in keeping Dirac strings hidden. It would therefore still be important to find approximate superpositions that achieve this. Nevertheless, it shows how subtle it is to consider Abelian fields as embedded in non-Abelian ones. There is much more to 't Hooft's Abelian projection [7] than meets the eye at first glance.

The rest of the paper will be organized as follows. In Section 2 we formulate the Fourier analysis of the ADHM data for calorons of higher charge. This allows us in Section 2.1 to relate to the Nahm equations, providing the connection between the ADHM and Nahm data. The Nahm equation for charge k calorons [4] expresses self-duality of dual $SU(k)$ gauge fields on a circle, but with singularities. In Section 2.2 we introduce the “master” Green's function in terms of which the gauge field (Section 2.3) and the action density (Section 2.4) can be explicitly computed, relying heavily on some beautiful results [8,9] derived in the context of the ADHM construction.

This can all be achieved without explicitly solving the Nahm equation. In Section 3 we will, however, solve it for some special cases with axial symmetry. There we also illustrate some interesting features that appear when constituents overlap, similar to what was observed at zero temperature [10].

Section 4 is devoted to the far-field limit (related to the high-temperature limit), where up to exponential corrections only the Abelian component of the field survives. Again, expressions can be derived without explicitly solving the Nahm equation. We apply the formalism to the exact axially symmetric solutions in Section 4.3.1, where we prove that in the far-field region they are in a precise sense described by (self-dual) Dirac monopoles, which is conjectured to be the case for any exact solution.

We end in Section 5 with a discussion of lattice results that have been obtained by various groups, some open questions and suggestions for future studies.

2. Construction

In constructing the higher charge caloron solutions similar steps are followed as for charge 1. We distinguish two constructions, $Sp(n)$ based on quaternions, and $SU(n)$ based on complex spinors. With $SU(2) = Sp(1)$, this implies that for $SU(2)$ two constructions are possible. For $k = 1$ it was easily shown these are identical, but for $k > 1$ this is more complicated due to the quadratic ADHM constraint [3] which cannot be solved in all

generality. Since the essential part of the construction that employs the impurity scattering technique is identical in both approaches, we will give a unified presentation.

The $SU(n)$ ADHM formalism for charge k instantons [3] employs a k -dimensional vector $\lambda = (\lambda_1, \dots, \lambda_k)$, where λ_i^\dagger is a two-component spinor in the \bar{n} representation of $SU(n)$. Alternatively, λ can be seen as a $n \times 2k$ complex matrix. In addition one has four complex Hermitian $k \times k$ matrices B_μ , combined into a $2k \times 2k$ complex matrix $B = \sigma_\mu \otimes B_\mu$, using the unit quaternions $\sigma_\mu = (\mathbb{1}_2, i\vec{\tau})$ and $\bar{\sigma}_\mu = (\mathbb{1}_2, -i\vec{\tau})$, where τ_i are the Pauli matrices. With some abuse of notation, we often write $B = \sigma_\mu B_\mu$. Together λ and B constitute the $(n + 2k) \times 2k$ dimensional matrix $\Delta(x)$, to which is associated a complex $((n + 2k) \times n)$ -dimensional normalized zero mode vector $v(x)$,

$$\Delta(x) = \begin{pmatrix} \lambda \\ B(x) \end{pmatrix}, \quad B(x) = B - x, \quad \Delta^\dagger(x)v(x) = 0, \quad v^\dagger(x)v(x) = \mathbb{1}_n. \quad (2)$$

Here the quaternion $x = x_\mu \sigma_\mu$ denotes the position (a $k \times k$ unit matrix is implicit) and $v(x)$ can be solved explicitly in terms of the ADHM data by

$$v(x) = \begin{pmatrix} -\mathbb{1}_n \\ u(x) \end{pmatrix} \phi^{-\frac{1}{2}}, \quad u(x) = (B^\dagger - x^\dagger)^{-1} \lambda^\dagger, \quad \phi(x) = \mathbb{1}_n + u^\dagger(x)u(x). \quad (3)$$

As $\phi(x)$ is an $n \times n$ positive Hermitian matrix, its square root $\phi^{\frac{1}{2}}(x)$ is well-defined. The gauge field is given by

$$A_\mu(x) = v^\dagger(x) \partial_\mu v(x) = \phi^{-\frac{1}{2}}(x) (u^\dagger(x) \partial_\mu u(x)) \phi^{-\frac{1}{2}}(x) + \phi^{\frac{1}{2}}(x) \partial_\mu \phi^{-\frac{1}{2}}(x). \quad (4)$$

The $Sp(1)$ ADHM formalism for charge k instantons [3] employs also a k -dimensional vector $\lambda = (\lambda_1, \dots, \lambda_k)$, where now λ_i is a quaternion (4 real parameters). Again, λ can be seen as an $2 \times 2k$ complex matrix (but with $4k$ real, as opposed to complex, parameters). Now the four $k \times k$ matrices B_μ are required to be real and symmetric, still to be combined into a $2k \times 2k$ complex matrix $B = \sigma_\mu B_\mu$. The $(2 + 2k) \times 2k$ dimensional matrix $\Delta(x)$ is constructed as before. It is immediately obvious that now $\phi(x)$ is proportional to σ_0 , simplifying the expression for the gauge field to

$$A_\mu(x) = v^\dagger(x) \partial_\mu v(x) = (u^\dagger(x) \partial_\mu u(x)) / \phi(x). \quad (5)$$

For $A_\mu(x)$ to be a self-dual connection, $\Delta(x)$ has to satisfy the quadratic ADHM constraint, which states that $\Delta^\dagger(x)\Delta(x) = B^\dagger(x)B(x) + \lambda^\dagger\lambda$ (considered as a $k \times k$ complex quaternionic matrix) has to commute with the quaternions, or equivalently

$$\Delta^\dagger(x)\Delta(x) = \sigma_0 \otimes f_x^{-1}, \quad (6)$$

defining f_x as a Hermitian (resp. symmetric) $k \times k$ Green's function. The self-duality follows by computing the curvature

$$F_{\mu\nu} = 2\phi^{-\frac{1}{2}}(x) u^\dagger(x) \eta_{\mu\nu} f_x u(x) \phi^{-\frac{1}{2}}(x), \quad (7)$$

making essential use of the fact that f_x commutes with the quaternions, and $\eta_{\mu\nu} \equiv \sigma_{[\mu} \bar{\sigma}_{\nu]}$ being self-dual ($\bar{\eta}_{\mu\nu} \equiv \bar{\sigma}_{[\mu} \sigma_{\nu]}$ is anti-self dual). The quadratic constraint can be formulated

as $\Im(\Delta^\dagger(x)\Delta(x)) = 0$, where $\Im W \equiv W - \frac{1}{2}\sigma_0 \text{tr}_2 W$, and one obtains

$$\bar{\eta}_{\mu\nu} \otimes B_\mu B_\nu + \frac{1}{2}\tau_a \otimes \text{tr}_2(\tau_a \lambda^\dagger \lambda) = 0, \quad (8)$$

where tr_2 is the spinorial trace. Note that this implies that $\text{tr}_2(\tau_a \lambda^\dagger \lambda)$ is traceless for $a = 1, 2, 3$.

To count the number of instanton parameters we observe that the transformation $\lambda \rightarrow \lambda T^\dagger$, $B_\mu \rightarrow T B_\mu T^\dagger$, with $T \in U(k)$ (respectively, $T \in O(k)$) leaves the gauge field and the ADHM constraint untouched. Taking this symmetry into account, one checks the dimension of the instanton moduli space to be $4kn$ dimensional. We have $4kn$ and $4k^2$ real parameters from λ and B_μ . The $U(k)$ symmetry removes k^2 real parameters and finally the quadratic ADHM constraint gives $3k^2$ real equations. On the other hand, for the quaternionic construction there are $4k$ and $4 \cdot \frac{1}{2}k(k+1)$ parameters from λ and B_μ , of which $\frac{1}{2}k(k-1)$ are removed by the $O(k)$ symmetry, and the quadratic ADHM constraint gives $3 \cdot \frac{1}{2}k(k-1)$ equations. Global gauge transformations are realized by $\lambda \rightarrow g\lambda$, with $g \in SU(n)$ and are here included in the parameter count. For calorons with non-trivial holonomy the dimension of the gauge invariant parameter space is minimally reduced by $n-1$ (maximal symmetry breaking) and maximally by n^2-1 (trivial holonomy).

We note that for $SU(2)$ the quadratic ADHM constraint and symmetry of the ADHM data for high charge differ considerably. For the caloron we have to deal in a sense with infinite topological charge, but finite within each (imaginary) time interval of length β . This infinity is resolved by Fourier transformation, relating it to the Nahm formalism [4], but the difference between the $U(k)$ and $O(k)$ symmetries (the infinity is moved to making these gauge symmetries local) remains, as well as of course the nature of the Nahm data (the Fourier transformation of the ADHM data). Henceforth we put $\beta = 1$, which can always be achieved by a rescaling.

Like for charge one [1,2] the caloron with Polyakov loop \mathcal{P}_∞ at infinity is built out of a periodic array of instantons, twisted by \mathcal{P}_∞ . This is implemented in the ADHM formalism by requiring (suppressing color and spinor indices, respectively, quaternion indices)

$$u_{pk+k+a}(x+1) = u_{pk+a}(x)\mathcal{P}_\infty^{-1} \quad (9)$$

with $p \in \mathbb{Z}$ (the Fourier index), and $a = 1, \dots, k$ (associated to the non-Abelian nature of the Nahm data). Using that $\phi^{\pm\frac{1}{2}}(x+1) = \mathcal{P}_\infty \phi^{\pm\frac{1}{2}}(x)\mathcal{P}_\infty^{-1}$, Eq. (4) leads to the required periodicity. Demanding

$$\lambda_{pk+k+a} = \mathcal{P}_\infty \lambda_{pk+a}, \quad B_{pk+a,qk+b} = B_{pk-k+a,qk-k+b} + \sigma_0 \delta_{pq} \delta_{ab}, \quad (10)$$

suitably implements Eq. (9) and is partially solved by imposing

$$\lambda_{pk+a} = \mathcal{P}_\infty^p \zeta_a, \quad B_{pk+a,qk+b} = p\sigma_0 \delta_{pq} \delta_{ab} + \hat{A}_{p-q}^{ab}, \quad (11)$$

with \hat{A} still to be determined to account for Eq. (8). It is useful to introduce the n projectors P_m on the m th eigenvalue of \mathcal{P}_∞ , such that $\mathcal{P}_\infty = \sum_m e^{2\pi i \mu_m} P_m$ and $\lambda_{pk+a} = \sum_m e^{2\pi i p \mu_m} P_m \zeta_a$.

2.1. Nahm setting

We now perform the Fourier transformation to the Nahm setting [4], which casts B into a Weyl operator and $\lambda^\dagger \lambda$ into a singularity structure on S^1 ,

$$\begin{aligned} \sum_{p,q} B_{pk+a,qk+b}(x) e^{2\pi i(pz-qz')} &= \frac{\delta(z-z')}{2\pi i} \widehat{D}^{ab}(z'), \\ 2\pi i \sum_p e^{2\pi i p z} \hat{A}_p^{ab} &= \hat{A}^{ab}(z), \\ \sum_{p,q} \lambda_{pk+a}^\dagger e^{2\pi i(pz-qz')} \lambda_{qk+b} &= \delta(z-z') \hat{\Lambda}_{ab}(z), \quad \sum_p e^{-2\pi i p z} \lambda_{pk+a} = \hat{\lambda}_a(z). \end{aligned} \quad (12)$$

With $B = \sigma_\mu B^\mu$, we can write $\widehat{D}(z) = \sigma_\mu \widehat{D}^\mu(z)$ and $\hat{A}(z) = \sigma^\mu \hat{A}_\mu(z)$, where

$$\begin{aligned} \widehat{D}_x^{ab}(z) &\equiv \widehat{D}^{ab}(z) - 2\pi i x \delta^{ab} = \delta^{ab} \left(\sigma_0 \frac{d}{dz} - 2\pi i x \right) + \hat{A}^{ab}(z), \\ \hat{\Lambda}_{ab}(z) &= \sum_m \delta(z - \mu_m) \zeta_a^\dagger P_m \zeta_b, \quad \hat{\lambda}_a(z) = \sum_m \delta(z - \mu_m) P_m \zeta_a. \end{aligned} \quad (13)$$

It should be noted that B_μ Hermitian, implies that $\hat{A}_\mu(z)$ is Hermitian (as a $k \times k$ matrix), whereas a real symmetric B_μ in addition implies $\hat{A}_\mu^t(z) = \hat{A}_\mu(-z)$.

The 2×2 matrix \hat{A}^{ab} can always be decomposed as

$$\zeta_a^\dagger P_m \zeta_b = \frac{1}{2\pi} (\sigma_0 \widehat{S}_m^{ab} - \vec{\tau} \cdot \vec{\rho}_m^{ab}). \quad (14)$$

On the diagonal one can show, as for $k = 1$, that $\widehat{S}_m^{aa} = |\vec{\rho}_m^{aa}|$, but in general the relation between $\vec{\rho}_m$ and \widehat{S}_m is more complicated,

$$\widehat{S}_m^{ab} \widehat{S}_m^{cd} + \widehat{S}_m^{ad} \widehat{S}_m^{cb} = \vec{\rho}_m^{ab} \cdot \vec{\rho}_m^{cd} + \vec{\rho}_m^{ad} \cdot \vec{\rho}_m^{cb}. \quad (15)$$

Furthermore, $\text{tr}_2(\vec{\tau} \lambda^\dagger \lambda)$ is traceless implies that $\sum_{a=1}^k \sum_{m=1}^n \vec{\rho}_m^{aa} = \vec{0}$. Both these conditions are equally valid for the $Sp(1)$ construction. But in the latter case, since through the Nahm equation $\vec{\rho}_m$ determines the discontinuities in $\hat{A}(z)$, compatibility with $\hat{A}_\mu^t(z) = \hat{A}_\mu(-z)$ requires $\vec{\rho}_1 + \vec{\rho}_2^t = \vec{0}$, which will be verified below Eq. (19). The Nahm equation is obtained by Fourier transforming the quadratic ADHM constraint

$$\frac{1}{2} [\widehat{D}_\mu(z), \widehat{D}_\nu(z)] \bar{\eta}_{\mu\nu} = 4\pi^2 \Im \hat{\Lambda}(z), \quad (16)$$

or in more familiar form (as a $k \times k$ matrix equation)

$$\begin{aligned} \frac{d}{dz} \hat{A}_j(z) + [\hat{A}_0(z), \hat{A}_j(z)] + \frac{1}{2} \varepsilon_{jkl} [\hat{A}_k(z), \hat{A}_l(z)] &= 2\pi i \sum_m \delta(z - \mu_m) \rho_m^j, \\ \hat{A}_j : & \begin{array}{ccccccc} \rho_1^j & \rho_2^j & \rho_3^j & \cdots & \rho_{n-2}^j & \rho_{n-1}^j & \rho_n^j & \rho_1^j \\ \downarrow & \downarrow & \downarrow & & \downarrow & \downarrow & \downarrow & \downarrow \\ z = \mu_1 & \mu_2 & \mu_3 & & \mu_{n-2} & \mu_{n-1} & \mu_n & \mu_{n+1} \equiv \mu_1 + 1 \end{array} \end{aligned} \quad (17)$$

where the figure illustrates the jumps of \hat{A}_j at each of the singularities (an overall factor of $2\pi i$ is not shown). The T symmetry in the ADHM construction translates into a $U(k)$ gauge symmetry on S^1 , which allows one to set $\hat{A}_0 = 2\pi i \xi_0$ to be constant, where ξ_0 is a Hermitian matrix which can be made diagonal by a constant gauge transformation. Its trace part can be absorbed in x_0 .

2.2. Green's function

Central to the ADHM construction is the Green's function f_x , which when Fourier transformed to $\hat{f}_x^{ab}(z, z') \equiv \sum_{p,q} f_x^{pk+a, qk+b} e^{2\pi i(pz - qz')}$ is a solution to the differential equation

$$\left\{ \left(\frac{\hat{D}_x^\mu(z)}{2\pi i} \right)^2 + \frac{1}{2\pi} \sum_m \delta(z - \mu_m) \hat{S}_m \right\} \hat{f}_x(z, z') = \mathbb{1}_k \delta(z - z'),$$

$$\frac{d\hat{f}_x}{dz} : \begin{array}{cccccccccccc} & \hat{S}_1 & & \hat{S}_2 & & \hat{S}_3 & & 2\pi \mathbb{1}_k & & \hat{S}_{n-2} & \hat{S}_{n-1} & \hat{S}_n & \hat{S}_1 \\ - & \downarrow & - & \downarrow & - & \downarrow & - & \downarrow & - & \downarrow & \downarrow & \downarrow & - \\ z = \mu_1 & & \mu_2 & & \mu_3 & & z' & & \mu_{n-2} & \mu_{n-1} & \mu_n & \mu_{n+1} \equiv \mu_1 + 1 \end{array} \quad (18)$$

where the figure illustrates the jumps for the *derivative* of \hat{f}_x (itself being continuous) at each of the singularities, which now includes $z = z'$ (an overall factor of 2π is omitted). With help of the impurity scattering formalism we will be able to express the solution in a simple form, without assuming explicit knowledge of $\hat{A}(z)$. As a bonus this also gives a more transparent derivation for $k = 1$. The equation for the Green's function is valid for the $SU(n)$ and $Sp(1)$ formulations alike. In general the matrix f_x is complex Hermitian, but for $Sp(1)$ it is real symmetric, which implies that

$$\hat{f}_x^{ab}(z, z') = \hat{f}_x^{ba}(z', z)^*, \quad \text{and for } Sp(1) \text{ only } \hat{f}_x^{ab}(z, z') = \hat{f}_x^{ba}(-z', -z). \quad (19)$$

For $Sp(1)$ consistency requires, $\hat{S}_1 - \hat{S}_2^j = 0$, which is to be compared with the condition we found in the previous section, $\bar{\rho}_1 + \bar{\rho}_2^j = 0$. To demonstrate the validity of these relations we make use of the fact that $\zeta_a = \zeta_a^\mu \sigma_\mu$, with ζ_a^μ real (such that $\zeta_a^\dagger = \bar{\zeta}_a$). Furthermore, we note that with $\mathcal{P}_\infty \equiv \exp(2\pi i \hat{\omega} \cdot \vec{\tau})$, $\mu_2 = -\mu_1 = \omega \equiv |\vec{\omega}|$, whereas $P_1 = \frac{1}{2}(\mathbb{1}_2 - \hat{\omega} \cdot \vec{\tau})$ and $P_2 = \frac{1}{2}(\mathbb{1}_2 + \hat{\omega} \cdot \vec{\tau})$. Introducing $\Omega \equiv \hat{\omega} \cdot \vec{\sigma} = i \hat{\omega} \cdot \vec{\tau}$, which is an imaginary unit quaternion (i.e., $\bar{\Omega} = -\Omega$, $\bar{\Omega} \Omega = \sigma_0$), we find with the help of Eq. (14)

$$\begin{aligned} & \sigma_0 \hat{S}_m^{ab} - \vec{\tau} \cdot \vec{\rho}_m^{ab} \\ &= \pi \zeta_a^\mu \bar{\sigma}_\mu (\sigma_0 - i(-1)^m \Omega) \zeta_b^\nu \sigma_\nu \\ &= \pi \zeta_a^\mu \zeta_b^\nu ([\bar{\sigma}_{[\mu} \sigma_{\nu]} - i(-1)^m \bar{\sigma}_{[\mu} \Omega \sigma_{\nu]}] + [\bar{\sigma}_{[\mu} \sigma_{\nu]} - i(-1)^m \bar{\sigma}_{[\mu} \Omega \sigma_{\nu]}]) \\ &= \sigma_0 \pi [\zeta_a^\mu \zeta_b^\mu - i(-1)^m \hat{\omega} \cdot \vec{\eta}_{\mu\nu} \zeta_a^\mu \zeta_b^\nu] + \pi [\bar{\eta}_{\mu\nu} \zeta_a^\mu \zeta_b^\nu + (-1)^m \bar{\zeta}_{[a} \hat{\omega} \cdot \vec{\tau} \zeta_{b]}], \end{aligned} \quad (20)$$

for which we used that $\bar{\sigma}_{[\mu} \Omega \sigma_{\nu]}$ is a real quaternion, therefore, given by

$$\frac{1}{2} \sigma_0 \text{tr}_2(\bar{\sigma}_{[\mu} \Omega \sigma_{\nu]}) = \frac{1}{2} \sigma_0 \text{tr}_2(\Omega \eta_{\nu\mu}) = \sigma_0 \hat{\omega} \cdot \vec{\eta}_{\nu\mu}.$$

We directly read off \widehat{S}_m and $\vec{\rho}_m$ and verify that indeed $\widehat{S}_1 = \widehat{S}_2^t$ and $\vec{\rho}_1 = -\vec{\rho}_2^t$. We wrote the result so as to easily make contact with the $k = 1$ results [1] (for which the 2nd term in \widehat{S}_m and the 1st term in $\vec{\rho}_m$ do not contribute).

In formulating the impurity scattering we note that the $U(k)$ gauge transformation

$$\hat{g}(z) = \exp(2\pi i(\xi_0 - x_0 \mathbb{1}_k)z) \quad (21)$$

turns $\widehat{D}_x^0(z)$ into the ordinary derivative and conjugates all other objects in Eq. (18), such that

$$\left\{ -\frac{d^2}{dz^2} + V(z; \vec{x}) \right\} f_x(z, z') = 4\pi^2 \mathbb{1}_k \delta(z - z'), \quad (22)$$

with $f_x(z, z')$ and $V(z; \vec{x})$ given by

$$\begin{aligned} f_x(z, z') &\equiv \hat{g}(z) \hat{f}_x(z, z') \hat{g}^\dagger(z'), \\ V(z; \vec{x}) &\equiv 4\pi^2 \vec{R}^2(z; \vec{x}) + 2\pi \sum_m \delta(z - \mu_m) S_m, \end{aligned} \quad (23)$$

where $\vec{R}(z; \vec{x})$ and S_m are defined by

$$R_j(z; \vec{x}) \equiv x_j \mathbb{1}_k - \frac{1}{2\pi i} \hat{g}(z) \hat{A}_j(z) \hat{g}^\dagger(z), \quad S_m \equiv \hat{g}(\mu_m) \widehat{S}_m \hat{g}^\dagger(\mu_m). \quad (24)$$

Periodicity is now only up to a gauge transformation. Note that $R_j(z; \vec{x})$ is a Hermitian $k \times k$ matrix, and that $V(z; \vec{x})$ does *not* depend on x_0 . By combining f_x and its derivative into a vector,

$$\vec{f}_x(z, z') \equiv \begin{pmatrix} f_x(z, z') \\ \frac{d}{dz} f_x(z, z') \end{pmatrix}, \quad (25)$$

we can turn the second order equation in to a first order equation

$$\left\{ \frac{d}{dz} - \begin{pmatrix} 0 & \mathbb{1}_k \\ V(z; \vec{x}) & 0 \end{pmatrix} \right\} \vec{f}_x(z, z') = \vec{C} \delta(z - z'), \quad \vec{C} \equiv -4\pi^2 \begin{pmatrix} 0 \\ \mathbb{1}_k \end{pmatrix}. \quad (26)$$

Its solution is

$$\begin{aligned} \vec{f}_x(z, z') &= W(z) [\vec{c}(z') - \theta(z' - z) W^{-1}(z') \vec{C}], \\ \frac{d}{dz} W(z) &= \begin{pmatrix} 0 & \mathbb{1}_k \\ V(z; \vec{x}) & 0 \end{pmatrix} W(z) \end{aligned} \quad (27)$$

where W is a 2×2 matrix, whereas \vec{c} is a two-component vector (like \vec{C}), all components being Hermitian $k \times k$ matrices. The theta function takes care of the inhomogeneous part of the equation. However, we have to restrict to $z' \in [z - 1, z + 1]$ since the delta function is periodic. The solution can be extended beyond this range using the periodicity, which when imposed, as we will see, also determines $\vec{c}(z')$.

The solution for $W(z)$ can be (formally) written as a path ordered exponential integral in the usual way. To show that this, indeed, makes sense, we should specify how to deal with the delta functions in V . From the definition of the path ordered exponential integral

we find $W(\mu_m + 0) = T_m W(\mu_m - 0)$ with

$$T_m \equiv P \exp \left[\int_{\mu_m - 0}^{\mu_m + 0} \begin{pmatrix} 0 & \mathbb{1}_k \\ V(z; \vec{x}) & 0 \end{pmatrix} dz \right] = \exp \begin{pmatrix} 0 & 0 \\ 2\pi S_m & 0 \end{pmatrix} = \begin{pmatrix} \mathbb{1}_k & 0 \\ 2\pi S_m & \mathbb{1}_k \end{pmatrix}, \quad (28)$$

which correctly reflects the matching conditions due to the “impurity” at $z = \mu_m$, since $f_x(z, z')$ is continuous across $z = \mu_m$, whereas the derivative jumps with $2\pi S_m f_x(\mu_m, z')$ and both conditions can be summarized by $\vec{f}_x(\mu_m + 0, z') = T_m \vec{f}_x(\mu_m - 0, z')$. Note that \vec{f}_x evolves with z as $\vec{f}_x(z_2, z') = W(z_2) W^{-1}(z_1) \vec{f}_x(z_1, z')$, with

$$W(z_2) W^{-1}(z_1) = P \exp \left[\int_{z_1}^{z_2} \begin{pmatrix} 0 & \mathbb{1}_k \\ V(z; \vec{x}) & 0 \end{pmatrix} dz \right] \equiv W(z_2, z_1). \quad (29)$$

In particular, when $z_1 = \mu_m$ and $z_2 = \mu_{m+1}$ this gives the “propagation” between two neighboring impurities and we can write

$$H_m \equiv W(\mu_{m+1} - 0, \mu_m + 0) = P \exp \left[\int_{\mu_m}^{\mu_{m+1}} \begin{pmatrix} 0 & \mathbb{1}_k \\ 4\pi^2 \vec{R}^2(z; \vec{x}) & 0 \end{pmatrix} dz \right]. \quad (30)$$

Neither T_m nor H_m require us to specify a boundary condition for $W(z)$. A change in boundary condition, however, affects $\vec{c}(z')$. To avoid such ambiguities, we define $\vec{c}_{z_0}(z') \equiv W(z_0) \vec{c}(z')$ such that

$$\vec{f}_x(z, z') = W(z, z_0) [\vec{c}_{z_0}(z') - \theta(z' - z) W^{-1}(z', z_0) \vec{C}]. \quad (31)$$

We determine $\vec{c}_{z_0}(z')$ by scattering “around” the circle determined from the boundary conditions of \vec{f}_x . Using Eq. (23), the fact that $\hat{f}_x(z, z')$ is strictly periodic and that $\hat{g}(z + 1) = \hat{g}(1) \hat{g}(z)$, one finds $\vec{f}_x(z, z' + 1) = \vec{f}_x(z, z') \hat{g}^\dagger(1)$ and $\vec{f}_x(z + 1, z') = \hat{g}(1) \vec{f}_x(z, z')$ (where the order of the *matrix* multiplication, defined componentwise, is important). The latter condition can be used to fix $\vec{c}_{z_0}(z')$ over the range of one period, $z' \in [z, 1 + z]$ (the use of $\hat{f}_x(z, z')$ requires $z' \in [z - 1, z + 1]$, that of $\hat{f}_x(z + 1, z')$ further restricts the range for z' to $z' > z$). With the help of the periodicity properties of W it gives $\vec{c}_{z_0}(z') = (\mathbb{1}_{2k} - \hat{g}^\dagger(1) W(z_0 + 1, z_0))^{-1} W^{-1}(z', z_0) \vec{C}$. We thus find for *arbitrary* z_0

$$\vec{f}_x(z, z') = W(z, z_0) \{ (\mathbb{1}_{2k} - \mathcal{F}_{z_0})^{-1} - \theta(z' - z) \mathbb{1}_{2k} \} W^{-1}(z', z_0) \vec{C}, \quad (32)$$

where we introduced the “holonomy” \mathcal{F}_{z_0}

$$\mathcal{F}_{z_0} \equiv \hat{g}^\dagger(1) W(z_0 + 1, z_0) = g^\dagger(1) P \exp \left[\int_{z_0}^{1+z_0} \begin{pmatrix} 0 & \mathbb{1}_k \\ V(z; \vec{x}) & 0 \end{pmatrix} dz \right]. \quad (33)$$

The equation for \vec{f}_x is valid for $z' \in [z, z + 1]$, but can be extended with the appropriate periodicity specified above. We note that $\hat{g}^\dagger(1)$ plays the role of a cocycle, in the gauge where $\hat{A}_0(z) - 2\pi i x_0 \mathbb{1}_k$ is transformed to 0, with \mathcal{F}_{z_0} the full circle “scattering” matrix.

The z_0 -independence of \vec{f}_x follows from

$$\begin{aligned}\mathcal{F}_{z_0} &= g^\dagger(1)W(z_0+1, z'_0+1)W(z'_0+1, z_0) = W(z_0, z'_0)g^\dagger(1)W(z'_0+1, z_0) \\ &= W(z_0, z'_0)\mathcal{F}_{z'_0}W^{-1}(z_0, z'_0).\end{aligned}\quad (34)$$

Putting things together we, therefore, find

$$\begin{aligned}\hat{f}_x(z, z') &= \hat{g}^\dagger(z)(\mathbb{1}_k, 0) \cdot \vec{f}_x(z, z')\hat{g}(z'), \\ \widehat{D}_x^0(z)\hat{f}_x(z, z') &= \hat{g}^\dagger(z)(0, \mathbb{1}_k) \cdot \vec{f}_x(z, z')\hat{g}(z'),\end{aligned}\quad (35)$$

satisfying all required conditions as can be checked explicitly.

Interestingly, Eq. (34) implies $\mathcal{F}_{z_0+1} = \hat{g}(1)\mathcal{F}_{z_0}\hat{g}^\dagger(1)$ as should of course be the case. In the light of this we also note that (choosing $z_0 = \mu_m + 0$)

$$\begin{aligned}\mathcal{F}_{\mu_m} &= \hat{g}^\dagger(1)T_{m+n}H_{m+n-1}T_{m+n-1}H_{m+n-2}\cdots T_{m+1}H_m \\ &= T_mH_{m-1}\cdots T_2H_1T_1\hat{g}^\dagger(1)H_nT_nH_{n-1}\cdots T_{m+1}H_m, \\ \mathcal{F}_{\mu_m} : & \begin{array}{ccccccc} & T_m & & T_{m-1} & & T_1\hat{g}^\dagger(1) & & T_n & & T_{m+1} & & H_m \\ & \downarrow & & \downarrow & & \downarrow & & \downarrow & & \downarrow & & \downarrow \\ z = 1+\mu_m & & 1+\mu_{m-1} & & 1+\mu_1 & & \mu_n & & \mu_{m+1} & & \mu_m \end{array}\end{aligned}\quad (36)$$

using for the second identity that $T_{m+n} = \hat{g}(1)T_m\hat{g}^\dagger(1)$ and $H_{m+n} = \hat{g}(1)H_m\hat{g}^\dagger(1)$. We will use these ingredients further on to relate to the earlier results for $k=1$, where the positioning of $\hat{g}^\dagger(1)$ is of course irrelevant.

2.3. Gauge field

The central role of the Green's function $\hat{f}_x(z, z')$ becomes clear when one appeals to the fact that it can be used to find the gauge field (working out Eq. (4)), whereas its determinant gives a simple expression for the action density. This follows from the general ADHM construction [8,9], and can be directly taken over for the caloron [1,2,11]. For the gauge field one finds

$$\begin{aligned}A_\mu(x) &= \frac{1}{2}\phi^{1/2}(x)\lambda\bar{\eta}_{\mu\nu}\partial_\nu f_x\lambda^\dagger\phi^{1/2}(x) + \frac{1}{2}[\phi^{-1/2}(x), \partial_\mu\phi^{1/2}(x)] \\ &= \frac{1}{2}\phi^{1/2}(x)\bar{\eta}_{\mu\nu}^j\partial_\nu\phi_j(x)\phi^{1/2}(x) + \frac{1}{2}[\phi^{-1/2}(x), \partial_\mu\phi^{1/2}(x)],\end{aligned}\quad (37)$$

where $\phi(x)$ and $\phi_j(x)$ are $n \times n$ matrices defined by

$$\phi(x) \equiv (\mathbb{1}_n - \lambda f_x \lambda^\dagger)^{-1}, \quad \phi_j \equiv \lambda \sigma_j f_x \lambda^\dagger. \quad (38)$$

To apply this to the caloron all we have to do is perform the Fourier transformation,

$$\begin{aligned}\phi(x)^{-1} &= \mathbb{1}_n - \sum_{m,m'} P_m \zeta_a \hat{f}_x^{ab}(\mu_m, \mu_{m'}) \zeta_b^\dagger P_{m'}, \\ \phi_j &= \sum_{m,m'} P_m \zeta_a \sigma_j \hat{f}_x^{ab}(\mu_m, \mu_{m'}) \zeta_b^\dagger P_{m'}.\end{aligned}\quad (39)$$

For the $Sp(1)$ construction $\phi(x)$ is a real quaternion, and hence a multiple of σ_0 , after which the gauge field simplifies to

$$A_\mu(x) = \frac{1}{2}\phi(x)\bar{\eta}_{\mu\nu}^j\partial_\nu\phi_j(x). \quad (40)$$

To simplify $\phi(x)$ and $\phi_j(x)$ we use Eq. (19), together with $\mu_1 = -\mu_2$, such that $\hat{f}_x^{ab}(\mu_1, \mu_1) = \hat{f}_x^{ba}(\mu_2, \mu_2)$ and $\hat{f}_x^{ab}(\mu_1, \mu_2) = \hat{f}_x^{ba}(\mu_1, \mu_2) = \hat{f}_x^{ba}(\mu_2, \mu_1)^*$. We note that $\phi(x)$ and $\phi_j(x)$ involve the combinations $\zeta_a\sigma_\mu\bar{\zeta}_b^\dagger = \zeta_a\sigma_\mu\bar{\zeta}_b$, which can be split in symmetric and anti-symmetric combinations (cf. Eq. (20))

$$\zeta_a\sigma_0\bar{\zeta}_b = \sigma_0\zeta_a^\mu\zeta_b^\mu + \eta_{\mu\nu}\zeta_a^\mu\zeta_b^\nu, \quad \zeta_a\sigma_j\bar{\zeta}_b = \sigma_0\bar{\eta}_{\mu\nu}^j\zeta_a^\mu\zeta_b^\nu + \zeta_{[a}\sigma_j\bar{\zeta}_{b]}. \quad (41)$$

No contributions from $\hat{f}_x^{ab}(\mu_1, \mu_2)$ and $\hat{f}_x^{ab}(\mu_2, \mu_1)$ can appear in $\phi(x)$ since these are symmetric in a and b , selecting from $\zeta_a\sigma_0\bar{\zeta}_b$ the term proportional to σ_0 , but $P_1\sigma_0P_2$ and $P_2\sigma_0P_1$ vanish. Therefore (cf. Eq. (20))

$$\begin{aligned} \phi(x)^{-1} &= \sigma_0 - \hat{f}_x^{ab}(\mu_2, \mu_2) \sum_{m=1}^2 (P_m\zeta_a^\mu\zeta_b^\mu P_m + (-1)^m P_m\eta_{\mu\nu}\zeta_a^\mu\zeta_b^\nu P_m) \\ &= \sigma_0[1 - \hat{f}_x^{ab}(\mu_2, \mu_2)(\zeta_a^\mu\zeta_b^\mu + i\hat{\omega} \cdot \bar{\eta}_{\mu\nu}\zeta_a^\mu\zeta_b^\nu)] \\ &= \sigma_0[1 - \pi^{-1}\text{Tr}_k(\hat{f}_x(\mu_2, \mu_2)\hat{S}_2)]. \end{aligned} \quad (42)$$

Similarly we can simplify the expression for $\phi_j(x)$, which we split in a charged component and Abelian, or neutral, component $\phi_j(x) = \phi_j^{\text{ch}}(x) + \phi_j^{\text{abel}}(x)$ with

$$\phi_j^{\text{ch}} = \hat{f}_x^{ab}(\mu_1, \mu_2)P_1\zeta_{[a}\sigma_j\bar{\zeta}_{b]}P_2 - \text{h.c.} \quad (43)$$

and

$$\begin{aligned} \phi_j^{\text{abel}}(x) &= \hat{f}_x^{ab}(\mu_2, \mu_2) \sum_{m=1}^2 (P_m\zeta_{[a}\sigma_j\bar{\zeta}_{b]}P_m + (-1)^m P_m\bar{\eta}_{\mu\nu}^j\zeta_a^\mu\zeta_b^\nu P_m) \\ &= i\hat{\omega} \cdot \bar{\tau} \hat{f}_x^{ab}(\mu_2, \mu_2) \left[\frac{1}{2} \text{tr}_2(\hat{\omega} \cdot \bar{\tau} \zeta_{[a}\tau_j\bar{\zeta}_{b]}) - i\bar{\eta}_{\mu\nu}^j\zeta_a^\mu\zeta_b^\nu \right] \\ &= -i\hat{\omega} \cdot \bar{\tau} \pi^{-1} \text{Tr}_k(\hat{f}_x(\mu_2, \mu_2)\rho_2^j), \end{aligned} \quad (44)$$

where we used that $\frac{1}{2} \text{tr}_2(\hat{\omega} \cdot \bar{\tau} \zeta_{[a}\tau_j\bar{\zeta}_{b]}) = \frac{1}{2} \text{tr}_2(\bar{\zeta}_{[b}\hat{\omega} \cdot \bar{\tau} \zeta_{a]}\tau_j)$ to correctly identify $\vec{\rho}_2^{ba}$, see Eq. (20). We may of course express $\phi(x)$ and $\phi_j^{\text{abel}}(x)$ also in terms of the first impurity, $\phi^{-1}(x) = \sigma_0[1 - \pi^{-1} \text{Tr}_k(\hat{f}_x(\mu_1, \mu_1)\hat{S}_1)]$ and $\phi_j^{\text{abel}}(x) = i\hat{\omega} \cdot \bar{\tau} \pi^{-1} \text{Tr}_k(\hat{f}_x(\mu_1, \mu_1)\rho_1^j)$, as is easily verified.

Like for $k = 1$ we will show further on that $\hat{f}_x^{ab}(\mu_1, \mu_2)$ decays exponentially, away from the cores of the constituent monopoles, where only the Abelian component survives,

$$\begin{aligned} A_\mu^{\text{abel}}(x) &= -\frac{i}{2}\hat{\omega} \cdot \bar{\tau} [1 - \pi^{-1} \text{Tr}_k(\hat{f}_x(\mu_2, \mu_2)\hat{S}_2)]^{-1} \\ &\quad \times \bar{\eta}_{\mu\nu}^j \partial_\nu [\pi^{-1} \text{Tr}_k(\hat{f}_x(\mu_2, \mu_2)\rho_2^j)]. \end{aligned} \quad (45)$$

Note that for $k = 1$ we are able to write $A_\mu^{\text{abel}}(x) = -\frac{i}{2}\hat{\omega} \cdot \bar{\tau} e_j \bar{\eta}_{\mu\nu}^j \partial_\nu \log \phi(x)$, with $\vec{e} = \vec{\rho}_2/|\vec{\rho}_2|$, making use of the fact that $\hat{S}_m = |\vec{\rho}_m|$, but that this is no longer true for higher charge, despite the fact that on the diagonal we still have $\hat{S}_m^{aa} = |\vec{\rho}_m^{aa}|$. This seems to allow

for the dipoles of k well-separated calorons to point in different directions. We will discuss this issue further when studying the limiting behavior far from the cores of the constituents, where the field becomes algebraic and constituent locations are readily identified.

2.4. Action density

Within the ADHM formalism the action density is given by [9],

$$-\frac{1}{2} \text{Tr}_n F_{\mu\nu}^2(x) = -\frac{1}{2} \partial_\mu^2 \partial_\nu^2 \log \psi(x), \quad (46)$$

where $\psi(x)$ equals $1/\det(f_x)$ after regularization to extract an irrelevant overall and for calorons divergent constant. We will be able to find a simple expression for $\psi(x)$ at any k , generalizing the result for charge 1 calorons. We use that $\partial_\nu \log \det(f_x) = -\text{Tr}(\{\partial_\nu f_x^{-1}\} f_x) = \frac{1}{\pi i} \widehat{\text{Tr}}(\widehat{D}_x^\nu \hat{f}_x)$, where in the last step we performed the Fourier transformation, and $\widehat{\text{Tr}}$ includes an integration with respect to z . The case $\nu = 0$ is treated separately, due to the discontinuity in the z derivative of $\hat{f}_x(z, z')$ at $z = z'$, which we regularize using point-splitting:

$$\begin{aligned} & \frac{1}{\pi i} \widehat{\text{Tr}}(\widehat{D}_x^0 \hat{f}_x) \\ &= \lim_{\varepsilon \rightarrow 0} \frac{1}{2\pi i} \int_0^1 dz \text{Tr}_k \left(\frac{d}{dz} f_x(z + \varepsilon, z') + \frac{d}{dz} f_x(z - \varepsilon, z') \right)_{z'=z} \\ &= 4\pi i \int_0^1 dz \text{Tr} \left(W^{-1}(z, z_0) \begin{pmatrix} 0 & 0 \\ 0 & \mathbb{1}_k \end{pmatrix} W(z, z_0) \left[(\mathbb{1}_{2k} - \mathcal{F}_{z_0})^{-1} - \frac{1}{2} \mathbb{1}_{2k} \right] \right) \\ &= 2\pi i \int_0^1 dz \left[\text{Tr} \left((\mathbb{1}_{2k} - \mathcal{F}_{z_0})^{-1} - \frac{1}{2} \mathbb{1}_{2k} \right) - \frac{1}{4\pi^2} \frac{d}{dz} \text{Tr}_k(f_x(z, z)) \right]. \end{aligned} \quad (47)$$

The Tr without an index or hat indicates the full trace over the $2k \times 2k$ matrix involved. To see how the total derivative term appears (not contributing to the integral due to the periodicity of $\text{Tr}_k[f_x(z, z)]$) we use that

$$\begin{aligned} & \frac{d}{dz} \text{Tr}_k(\hat{f}_x(z, z)) \\ &= -4\pi^2 \frac{d}{dz} \text{Tr} \left(W^{-1}(z, z_0) \begin{pmatrix} 0 & 0 \\ \mathbb{1}_k & 0 \end{pmatrix} W(z, z_0) \left[(\mathbb{1}_{2k} - \mathcal{F}_{z_0})^{-1} - s \mathbb{1}_{2k} \right] \right) \\ &= -4\pi^2 \text{Tr} \left(W^{-1}(z, z_0) \left[\begin{pmatrix} 0 & 0 \\ \mathbb{1}_k & 0 \end{pmatrix}, \begin{pmatrix} 0 & \mathbb{1}_k \\ V(z; \vec{x}) & 0 \end{pmatrix} \right] \right. \\ & \quad \left. \times W(z, z_0) [(\mathbb{1}_{2k} - \mathcal{F}_{z_0})^{-1} - s \mathbb{1}_{2k}] \right) \\ &= -4\pi^2 \text{Tr} \left(W^{-1}(z, z_0) \begin{pmatrix} -\mathbb{1}_k & 0 \\ 0 & \mathbb{1}_k \end{pmatrix} W(z, z_0) [(\mathbb{1}_{2k} - \mathcal{F}_{z_0})^{-1} - s \mathbb{1}_{2k}] \right), \end{aligned} \quad (48)$$

with $s = 1/2$ (as for point-spitting, although one checks that the s dependent term actually vanishes). We note that \mathcal{F}_{z_0} depends on x_0 only through $\hat{g}(1)$, and that $\partial_0 \hat{g}(1) = 2\pi i \hat{g}(1)$, such that $\partial_0 \mathcal{F}_{z_0} = 2\pi i \mathcal{F}_{z_0}$. With this we find

$$\partial_0 \log \det(\hat{f}_x) = -\partial_0 \log \psi, \quad \psi \equiv \det(i e^{-\pi i x_0} (\mathbb{1}_{2k} - \mathcal{F}_{z_0}) / \sqrt{2}), \quad (49)$$

which is *independent* of z_0 . The factor $i/\sqrt{2}$ in the argument of the determinant was inserted just so ψ agrees with the definition introduced earlier for $k = 1$.

Next we compute $\partial_j \log \det(\hat{f}_x)$,

$$\begin{aligned} & \frac{1}{\pi i} \int_0^1 dz \operatorname{Tr}_k(\hat{D}_x^j \hat{f}_x(z, z)) \\ &= -2 \int_0^1 dz \operatorname{Tr}_k(R_j(z; \vec{x}) f_x(z, z)) \\ &= 8\pi^2 \int_0^1 dz \operatorname{Tr} \left(W^{-1}(z, z_0) \begin{pmatrix} 0 & 0 \\ R_j(z; \vec{x}) & 0 \end{pmatrix} W(z, z_0) [(\mathbb{1}_{2k} - \mathcal{F}_{z_0})^{-1} - s \mathbb{1}_{2k}] \right) \\ &= \operatorname{Tr} \left((\mathbb{1}_{2k} - \mathcal{F}_{z_0})^{-1} \mathcal{F}_{z_0} \int_{z_0}^{1+z_0} dz W^{-1}(z, z_0) \partial_j \begin{pmatrix} 0 & \mathbb{1}_k \\ V(z; \vec{x}) & 0 \end{pmatrix} W(z, z_0) \right), \quad (50) \end{aligned}$$

where again s can take any value, but for convenience is best set to 1 here. Finally noting that \mathcal{F}_{z_0} only depends on \vec{x} through $\vec{R}(z; \vec{x})$ and using that

$$W^{-1}(z, z_0) \partial_j W(z, z_0) = \int_{z_0}^{1+z_0} dz W^{-1}(z, z_0) \partial_j \begin{pmatrix} 0 & \mathbb{1}_k \\ V(z; \vec{x}) & 0 \end{pmatrix} W(z, z_0), \quad (51)$$

we verify that $\partial_\mu \log \det(\hat{f}_x) = -\partial_\mu \log \psi$ for all μ and k . It is amusing to note that this implies the remarkable formula

$$-\frac{1}{2} \operatorname{Tr}_n F_{\mu\nu}^2(x) = -\frac{1}{2} \partial_\mu^2 \partial_\nu^2 \log \det \left(\mathbb{1}_{2k} - \hat{g}^\dagger(1) P \exp \left[\int_0^1 \begin{pmatrix} 0 & \mathbb{1}_k \\ V(z; \vec{x}) & 0 \end{pmatrix} dz \right] \right), \quad (52)$$

even though explicit evaluation can be quite cumbersome. Not so for some special cases, including the single caloron $k = 1$, where $\vec{R}(z; \vec{x})$ is *piecewise constant* as we will discuss next.

3. Special cases

Consider $\vec{R}(z; \vec{x})$ to be piecewise constant, for $z \in [\mu_m, \mu_{m+1}]$ defined to be $\vec{x} - \vec{Y}_m$ (cf. Eq. (24)), with \vec{Y}_m constant Hermitian $k \times k$ matrices related to the Nahm potential by

$\hat{A}_j(z) = 2\pi i \hat{g}^\dagger(z) Y_m^j \hat{g}(z)$. In this case we can easily deal with the path ordered exponential integrals. To be specific, the “propagation” from μ_m to μ_{m+1} defined through H_m in Eq. (30), is given by

$$H_m = \begin{pmatrix} \cosh(2\pi v_m R_m) & (2\pi R_m)^{-1} \sinh(2\pi v_m R_m) \\ 2\pi R_m \sinh(2\pi v_m R_m) & \cosh(2\pi v_m R_m) \end{pmatrix}, \quad (53)$$

where $v_m = \mu_{m+1} - \mu_m$ (with $\mu_{m+n} = 1 + \mu_m$ such that $\sum_m v_m = 1$) and $R_m \equiv (\vec{R}_m \cdot \vec{R}_m)^{\frac{1}{2}}$ (a Hermitian $k \times k$ matrix). Since $\cosh(y)$ and $y^{\pm 1} \sinh(y)$ are both quadratic in y , actually no square root is involved in this expression for H_m .

3.1. The known charge 1-caloron

For charge 1 the Nahm equation (Eq. (17)) has no commutator terms and $\vec{R}(z; \vec{x})$ is always piecewise constant. It reduces to the m^{th} constituent radius for $z \in [\mu_m, \mu_{m+1}]$, $R_m = r_m \equiv |\vec{r}_m|$, whereas the prefactor at the impurity becomes $S_m = |\vec{r}_m - \vec{r}_{m-1}| = |\vec{\rho}_m|$. With

$$\mathcal{A}_m \equiv r_m^{-1} \begin{pmatrix} r_m & |\vec{\rho}_{m+1}| \\ 0 & r_{m+1} \end{pmatrix} \begin{pmatrix} \cosh(2\pi v_m r_m) & \sinh(2\pi v_m r_m) \\ \sinh(2\pi v_m r_m) & \cosh(2\pi v_m r_m) \end{pmatrix}, \quad (54)$$

a link to the earlier charge 1 results [2] is established by noting that

$$\mathcal{A}_m = \begin{pmatrix} 0 & 1 \\ 2\pi r_{m+1} & 0 \end{pmatrix} T_{m+1} H_m \begin{pmatrix} 0 & 1 \\ 2\pi r_m & 0 \end{pmatrix}^{-1}. \quad (55)$$

With the placing of $\hat{g}^\dagger(1)$ irrelevant, and the possibility of absorbing ξ_0 in x_0 , we therefore find

$$\mathcal{F}_{\mu_m}^{k=1} = \begin{pmatrix} 0 & 1 \\ 2\pi r_m & 0 \end{pmatrix} e^{2\pi i x_0} \mathcal{A}_{m-1} \mathcal{A}_{m-2} \cdots \mathcal{A}_1 \mathcal{A}_n \cdots \mathcal{A}_{m+1} \mathcal{A}_m \begin{pmatrix} 0 & 1 \\ 2\pi r_m & 0 \end{pmatrix}^{-1}, \quad (56)$$

cf. Eq. (36). In particular this shows that $\psi = -\frac{1}{2} e^{-2\pi i x_0} \det(\mathbb{1}_2 - \mathcal{F}_{\mu_m})$ agrees with the result found earlier, $\psi = \frac{1}{2} \text{tr}(\mathcal{A}_n \mathcal{A}_{n-1} \cdots \mathcal{A}_1) - \cos(2\pi x_0)$. The Green's functions can be shown to agree as well, using $(\mathbb{1}_2 - \mathcal{F}_{\mu_m})^{-1} = (\mathbb{1}_2 - \bar{\sigma}_2 \mathcal{F}_{\mu_m}^t \sigma_2) / \det(\mathbb{1}_2 - \mathcal{F}_{\mu_m})$.

3.2. Exact axially symmetric solution

Arranging $\vec{R}(z; \vec{x})$ to be piecewise constant when $k > 1$ requires one to fulfill some constraints. To solve the Nahm equation, Eq. (17), in terms of the $Y_m^j = \frac{1}{2\pi i} \hat{g}(z) \hat{A}_j(z) \hat{g}^\dagger(z)$, the commutator term should vanish. One way to achieve this, is by choosing $\vec{Y}_m = Y_m \vec{e}$. The Nahm equation relates the discontinuities of $\hat{A}_j(z)$ to $\vec{\rho}_m$,

$$\hat{g}^\dagger(\mu_m)(Y_m - Y_{m-1})\hat{g}(\mu_m)\vec{e} = \vec{\rho}_m, \quad (57)$$

which imposes constraints on ζ_a , see Eq. (14). To seek a solution we choose all ζ^a to be parallel in group space, $\zeta^a = \rho_a \zeta$ (ρ_a a positive real number). This reduces the problem

to $k = 1$, since $\zeta_a^\dagger P_m \zeta_b = \rho_a \rho_b \zeta^\dagger P_m \zeta$ is proportional to $\zeta^\dagger P_m \zeta$. For $SU(2)$ this already solves the constraint, since for $k = 1$ one has $\vec{\rho}_1 = -\vec{\rho}_2$. For $n > 2$ it has been shown [2] that $\vec{\rho}_m$ can take any value, provided $\sum_{m=1}^n \vec{\rho}_m = \vec{0}$, in particular we may choose all $\vec{\rho}_m$ to be proportional to \vec{e} (by properly choosing ζ). For $k = 1$ it is convenient to parametrize $\zeta^\dagger P_m \zeta = (|\vec{\rho}_m| - \vec{e} \cdot \vec{\rho}_m)/(2\pi)$ in terms of constituent locations, $\vec{\rho}_m = \Delta \vec{y}_m \equiv \vec{y}_m - \vec{y}_{m-1}$. As in Section 2.3 we will take $\vec{e} = \vec{\rho}_2/|\vec{\rho}_2|$.

We obtain a larger class of ζ^a for which the $\vec{\rho}_m$ are parallel, by taking ζ^a to be parallel up to a gauge rotation with an element of the unbroken subgroup $U(1)^{n-1} \subset SU(n)$ which leaves the holonomy unchanged,

$$\zeta_a = \rho_a \exp(2\pi i \alpha_a) \zeta, \quad \alpha_a \equiv \sum_{m=1}^n \alpha_a^m P_m, \quad \text{Tr}_n \alpha_a = 0. \quad (58)$$

This leads to

$$\vec{\rho}_m^{ab} = \rho^a \rho^b \exp(2\pi i (\alpha_b^m - \alpha_a^m)) \Delta \vec{y}_m, \quad \widehat{S}_m^{ab} = \vec{\rho}_m^{ab} \cdot \Delta \vec{y}_m / |\Delta \vec{y}_m|. \quad (59)$$

Note that for $Sp(1)$ we verify that $\vec{\rho}_1 + \vec{\rho}_2^t = \vec{0}$ and $\widehat{S}_1 - \widehat{S}_2^t = 0$ (using $\alpha_a^1 = -\alpha_a^2$). With $\Delta \vec{y}_m = \Delta y_m \vec{e}$ for all m (by definition $\Delta y_2 > 0$) we may solve Eq. (57),

$$Y_m^{ab} = (\xi_a + \rho_a^2 y_m) \delta_{ab} + i(1 - \delta_{ab}) \rho_a \rho_b \times \sum_{j=1}^n \Delta y_j \frac{\exp(2\pi i [\alpha_b^j - \alpha_a^j - (\mu_j + s_j^m)(\xi_0^b - \xi_0^a)])}{2 \sin(\pi [\xi_0^b - \xi_0^a])}, \quad (60)$$

where the ξ_a are arbitrary, $m = 1, \dots, n$ and $s_j^m = \frac{1}{2}$ for $j = 1, 2, \dots, m$ and $s_j^m = -\frac{1}{2}$ for $j = m+1, \dots, n$. The eigenvalues of these Hermitian matrices determine the constituent locations, all lined-up along \vec{e} . It should be noted that there is no reason to expect that all the Y_m can be diagonalized simultaneously. We will come back to this in the following section.

Returning to the simplest case of parallel gauge orientations, i.e., putting $\alpha_a^j = 0$, we may take the limit $\xi_0 \rightarrow 0$ (related to vanishing time separations) to find

$$Y_m^{ab} = (\xi_a + y_c \rho_a^2) \delta_{ab} + (y_m - y_c) \rho_a \rho_b, \quad y_c \equiv \sum_{m=1}^n y_m y_m. \quad (61)$$

The ($k = 1$) “center of mass” coordinate y_c can be freely chosen and the ξ^a play the role of “center of mass” of each constituent caloron. How exactly this is realized becomes clear when we diagonalize Y_m . Let us first consider Eq. (61) for $SU(2)$ and charge 2, $k = n = 2$, with $\xi_1 = -\xi_2 \equiv \xi$. Without loss of generality we choose $y_c = 0$, such that the two eigenvalues of Y_m are given by $y_m^{(j)} = \frac{1}{2} y_m \rho^2 + (-1)^j \sqrt{\xi^2 + \frac{1}{4} y_m^2 \rho^4 + y_m \xi \Delta \rho^2}$, where $\rho^2 \equiv \rho_1^2 + \rho_2^2$ and $\Delta \rho^2 \equiv \rho_1^2 - \rho_2^2$. For large and positive ξ we find $y_m^{(j)} = (-1)^j \xi + y_m \rho_j^2 + \mathcal{O}(\xi^{-1})$, representing two charge 1 calorons centered at ξ and $-\xi$, with separations between their constituents monopoles given in terms of $\Delta y_{2,1,2}$. We plot the constituent locations as a function of ξ in Fig. 3 for $y_2 = -y_1 = v_j = \frac{1}{2}$ and $\rho_j = 2$.

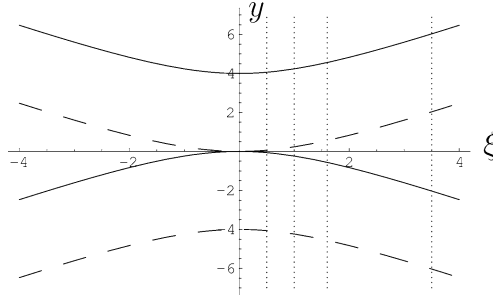


Fig. 3. Constituent locations $y_m^{(j)}$ based on Eq. (61) (i.e., $\alpha_a = 0$ and $\xi_0 \rightarrow 0$) as a function of $\xi = \xi_1 = -\xi_2$ for $y_2 = -y_1 = v_1 = v_2 = \frac{1}{2}$ and $\rho_1 = \rho_2 = 2$. Dashed versus full lines distinguish the magnetic charge of the constituents. The dotted lines represent the four cases shown in Figs. 2 and 4.

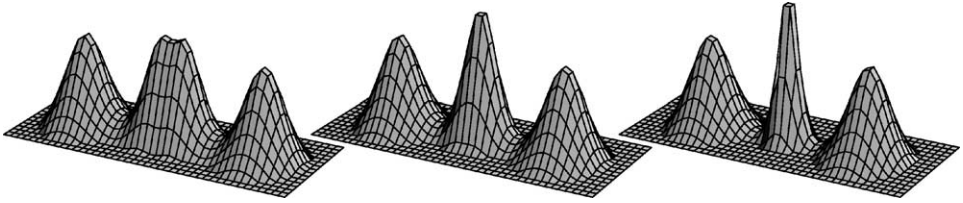


Fig. 4. The action density (cutoff for $\log(S)$ below -3) as a function of x and z for the $SU(2)$ solution with charge 2 ($\mu_2 = \frac{1}{4}$, $\alpha_a^j = \xi_0^a = 0$, $\rho_j = 2$) and increasing values of $\xi \equiv \xi_1 = -\xi_2$ (see Fig. 2 (left) for $\xi = 3.5$), with $\xi = 1.6$ (left), $\xi = 1.0$ (middle) and $\xi = 0.5$ (right). Compare Fig. 3 for the corresponding constituent locations.

Action density profiles are shown in Fig. 2 (left) for $\xi = 3.5$ and in Fig. 4 for $\xi = 1.6, 1.0, 0.5$. From the dotted lines in Fig. 3 one reads off the associated constituent locations. Note that the magnetic moments of the two calorons are pointing in the same direction and that we cannot freely interchange constituent monopole locations within our axially symmetric ansatz. However, when ξ is small it is more natural to interpret the configuration as a narrow caloron (i.e., instanton) with inverted magnetic moment in the background of a large caloron. This is the proper setting to understand the non-trivial time dependence for $\xi = 0.5$ illustrated in Fig. 5 (left).

For $\xi \rightarrow 0$ a singular caloron arises due to the fusion of two constituents (with opposite magnetic charge). This singularity is avoided when $\xi_0^a \neq 0$, which can be understood by observing that the eigenvalues of ξ_0^a parametrize time-locations. If $\alpha_a^j \neq 0$, with ξ_0 and ξ made small, one will find two calorons (and their constituents) to be pushed far from each other. This can be understood as well, in terms of a short-to-long distance duality in the ADHM data for an instanton pair with non-parallel group orientation [10], but can also be read off from the eigenvalues of Y_m defined in Eq. (60). As an example we take again $SU(2)$ and charge 2, but now with $\xi_0 \equiv \xi_0^1 = -\xi_0^2$ and $\alpha_1^2 = -\alpha_2^2 = -\alpha_1^1 = \alpha_2^1 \equiv \alpha$ in general non-zero. For the case $\alpha = 1/8$ (perpendicular relative color orientations), $\rho_1 = \rho_2 \equiv \rho$ and $\mu_2 = \frac{1}{4}$ (equal mass constituents), the eigenvalues are $y_m^{(j)} = y_m \rho^2 + (-1)^j \sqrt{\xi^2 + \frac{1}{4}(\Delta y_2)^2 \rho^4 \sin^{-2}(\pi \xi_0)}$, whereas for $\alpha = 0$ one finds $y_m^{(j)} =$

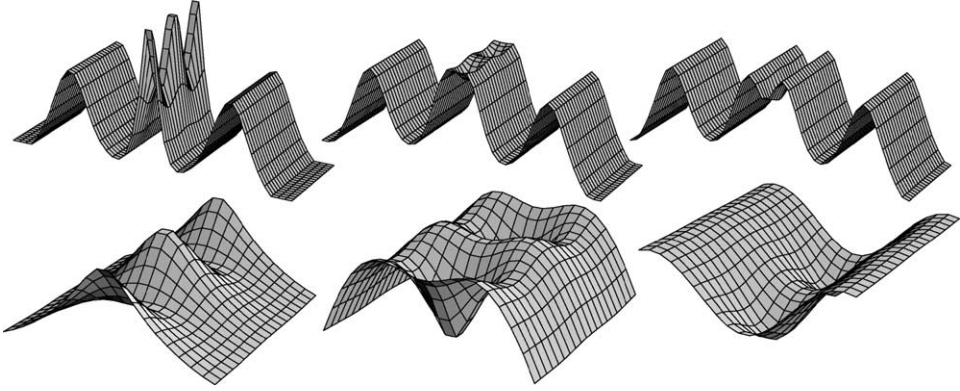


Fig. 5. The action density (cutoff for $\log(S)$ below -3) as a function of z and t (doubling the time-period) for the $SU(2)$ solution with charge 2 ($\mu_2 = \frac{1}{4}$, $\xi = \frac{1}{2}$, $\alpha_a^j = 0$, $\rho_j = 2$) and increasing values of ξ_0 , with $\xi_0 = 0$ (left), $\xi_0 = 0.2$ (middle) and $\xi_0 = 0.25$ (right), for the top row all on the same scale, zooming in on the middle region on the bottom row (not to scale). See Fig. 4 (right) for the case of $\xi_0 = 0$ shown as a function of x and z .

$y_m \rho^2 + (-1)^j \sqrt{\xi^2 + \frac{1}{4}(\Delta y_2)^2 \rho^4 \cos^{-2}(\pi \xi_0)}$. In the light of this it is interesting to observe, as shown in Fig. 5, that with $\alpha = 0$ and increasing ξ_0 the constituents are pushed out in the z direction as well. When $\xi_0 \rightarrow 0.5$ the constituents would otherwise come close together through the periodicity in the time direction. Effectively these constituents thus have perpendicular color orientations (due to our choice of holonomy with $\mu_2 = \frac{1}{4}$). The transition from constituents separating in the time direction for ξ_0 near 0 to constituents separating in the z direction for ξ_0 near $\frac{1}{2}$ occurs for $\rho = 2$ at approximately $\xi_0 = 0.2$.

With a little imagination one detects the ring-shaped structure also observed [10] in the case of instantons at zero temperature, see Fig. 5 (middle). A more direct analogy of course occurs when two calorons (with ρ small, i.e., instantons with unresolved constituent monopoles) approach each other. We checked that for $\xi = \alpha = 0$ and $\xi_0 \rightarrow 0$ a singular caloron forms due to the overlap of two calorons with parallel gauge orientations, whereas for $\xi_0 \rightarrow \frac{1}{2}$ the two calorons are pushed away (to infinity) in the z direction as is appropriate for the non-parallel group orientation due to the non-trivial holonomy. At an intermediate value ($\xi_0 = 0.25$ for $\rho_1 = \rho_2 = 0.1$) one observes a small ring in the t - z plane. Choosing ξ large one may check that $\pm \xi_0$ indeed gives the time location for each caloron. When, however, ξ_0 approaches $\frac{1}{2}$ they can no longer keep parallel gauge orientations due to the non-trivial holonomy. As noted before, this may be described by a solution with $\alpha \neq 0$ and $\xi_0 \rightarrow 0$. Computing the eigenvalues of Y_m therefore allows one to easily predict the behavior of the exact solution.

For charge 1 it had been shown [2] that as soon as one of the constituents is far removed from the others the solution becomes static. For the “dimensional reduction” to take place at higher charge this is no longer sufficient. We have seen (generalization to $SU(n)$ is straightforward) that any magnetically neutral cluster of constituents, when small with respect to β , will behave like an instanton that is localized in time. For the special case with parallel group orientations, putting all $\xi_a = 0$ in Eq. (61) one would even be left with $k - 1$ singular instantons on top of one regular caloron, whose scale parameter is set by

$\rho^2 = \sum_{a=1}^k \rho_a^2$, which can be understood from the fact that the matrix $\rho_a \rho_b$ has rank 1. It does, however, give us one opportunity to go beyond the axial symmetry considered so far. When $\xi_a = 0$ we could solve the Nahm equation for parallel gauge orientations by $\vec{Y}_m^{ab} = \vec{y}_m \rho_a \rho_b$ without insisting all the \vec{y}_m line-up. This still describes $k - 1$ singular instantons on top of one regular caloron, except that now the singular instantons can have arbitrary locations.

Even though our ansatz to obtain exact solutions has been restrictive (as is clear from the axial symmetry), we stress that the solutions for the Nahm equation we found provide genuine multi-caloron solutions, which reveal kn isolated lumps for each of its constituent monopoles (with suitably chosen ξ^a so the constituents do not overlap). This is not only illustrated in Fig. 2, but can also be understood analytically for any charge k and $SU(n)$ as follows. We diagonalize each Y_m with (in general *different*) similarity transformations U_m , or $Y_m \equiv U_m \text{diag}(y_m^{(1)}, \dots, y_m^{(k)}) U_m^\dagger$. These bring R_m to the diagonal form $R_m^{\text{diag}} = \text{diag}(r_m^{(1)}, \dots, r_m^{(k)})$, with $r_m^{(j)} \equiv |\vec{x} - y_m^{(j)} \vec{e}|$ the constituent radii, such that $\tilde{H}_m \equiv U_m^\dagger H_m U_m$ (U_m acting componentwise) simplifies to (cf. Eq. (53))

$$\tilde{H}_m \equiv \begin{pmatrix} \cosh(2\pi v_m R_m^{\text{diag}}) & (2\pi R_m^{\text{diag}})^{-1} \sinh(2\pi v_m R_m^{\text{diag}}) \\ 2\pi R_m^{\text{diag}} \sinh(2\pi v_m R_m^{\text{diag}}) & \cosh(2\pi v_m R_m^{\text{diag}}) \end{pmatrix}. \quad (62)$$

The action density can now be explicitly expressed in terms of the constituent radii

$$-\frac{1}{2} \text{Tr}_n F_{\mu\nu}^2(x) = -\frac{1}{2} \partial_\mu^2 \partial_\nu^2 \log \psi(x), \quad \psi = \det(i e^{-\pi i x_0} (\mathbb{1}_{2k} - \mathcal{F}) / \sqrt{2}),$$

$$\mathcal{F} \equiv \exp(2\pi i (x_0 \mathbb{1}_k - \xi_0)) U_n \tilde{H}_n \tilde{T}_n \tilde{H}_{n-1} \tilde{T}_{n-1} \cdots \tilde{H}_1 U_1^\dagger T_1 \quad (63)$$

cf. Eqs. (36), (46), (49), (53), where $\tilde{T}_m \equiv U_m^\dagger T_m U_{m-1}$ (U_m again acting componentwise). The size of the constituent monopoles is read off to be $(2\pi v_m)^{-1}$ (or $\beta(2\pi v_m)^{-1}$ when $\beta \neq 1$), and one concludes that the action density will contain kn lumps for sufficiently well separated constituents. The figures were produced by computing the action density using precisely this method.

4. Far-field limit

The non-trivial value of the Polyakov loop at spatial infinity (holonomy) leads to a spontaneous breaking of the gauge symmetry, but without the need of introducing a Higgs field. One may view A_0 as the Higgs field in the adjoint representation. This is one way to understand why constituent monopoles emerge. The best way to describe the caloron solutions, in case of well separated constituents, is by analyzing the field outside the cores of these constituents, where only the Abelian field survives. Since in our case the asymptotic Polyakov loop value defines a global direction in color space the Abelian generator in terms of which we can describe the so-called far-field configuration is fixed, giving rise to a global embedding in the full gauge group. Extrapolating the Abelian fields back to inside the core of the constituents leads to Dirac monopoles. Such an extrapolation is well defined in terms of the *high temperature limit*, which makes the core of the constituents shrink to zero size and the field to become a smooth Abelian gauge field

everywhere except for the singularities of the Dirac monopoles. Thus we anticipate that in this limit the self-dual Abelian field is still described by point like constituents, despite the fact that $\vec{R}(z, \vec{x})$ is no longer piecewise constant. Any “fuzziness” of the constituent location that may result from this, would be confined to the non-Abelian core, and not visible from afar.

4.1. Green's function

Despite the somewhat formal expression for the Green's function $\hat{f}_x(z, z')$, one can extract information about the long-range fields from it. In the following we will show how to neglect the exponentially decaying fields in the cores of the monopole constituents, being left with the Abelian components of fields which decay algebraically. We only need to consider the “bulk” contributions H_m , Eq. (30), which contain all the dependence on \vec{x} . Our starting point is Eq. (22) restricted to the m th interval, $z \in (\mu_m, \mu_{m+1})$

$$\left\{ -\frac{d^2}{dz^2} + 4\pi^2 \vec{R}^2(z; \vec{x}) \right\} f_m(z) = 0. \quad (64)$$

To distinguish between exponentially growing and decreasing contributions for this homogeneous equation we take as a basis for $f_m(z)$ functions $f_m^\pm(z)$ with the following asymptotic behavior

$$|\vec{x}| \rightarrow \infty: f_m^\pm(z) \rightarrow \exp(\pm 2\pi |\vec{x}| (z - \mu_m) \mathbb{1}_k), \quad (65)$$

relying on the fact that $\vec{R}^2(z; \vec{x}) \rightarrow \vec{x}^2 \mathbb{1}_k$. This prompts us to introduce on each interval the matrix valued functions $R_m^\pm(z)$ (we suppress the dependence on \vec{x}) such that

$$f_m^\pm(z) = P \exp \left[\pm 2\pi \int_{\mu_m}^z R_m^\pm(z) dz \right] \quad (66)$$

from which it follows that $R_m^\pm(z)$ is a solution of the Riccati equation

$$R_m^\pm(z)^2 \pm \frac{1}{2\pi} \frac{d}{dz} R_m^\pm(z) = \vec{R}^2(z; \vec{x}). \quad (67)$$

We note that for $|\vec{x}| \rightarrow \infty$, $R_m^\pm(z) \rightarrow |\vec{x}|$ and that for piecewise constant $\vec{R}(z; \vec{x})$ both $R_m^+(z)$ and $R_m^-(z)$ are constant and equal to R_m , introduced in Eq. (53).

We can write for $z, z' \in (\mu_m, \mu_{m+1})$ the “propagator” $W(z, z')$ defined in Eq. (29) in terms of $f_m^\pm(z)$ as $W(z, z') = W_m(z) W_m^{-1}(z')$ with

$$W_m(z) \equiv \begin{pmatrix} f_m^+(z) & f_m^-(z) \\ 2\pi R_m^+(z) f_m^+(z) & -2\pi R_m^-(z) f_m^-(z) \end{pmatrix}. \quad (68)$$

Using that $H_m = W_m(\mu_{m+1}) W_m^{-1}(\mu_m)$ and $f_m^\pm(\mu_m) = \mathbb{1}_k$, we find by neglecting the exponentially decreasing factors $f_m^-(\mu_{m+1})$ the required limiting behavior for H_m . Paying special attention to the ordering of the $k \times k$ matrices R_m^\pm , observing that

$$W_m^{-1}(\mu_m) = (4\pi R_m(\mu_m))^{-1} \begin{pmatrix} 2\pi R_m^-(\mu_m) & \mathbb{1}_k \\ 2\pi R_m^+(\mu_m) & -\mathbb{1}_k \end{pmatrix},$$

$$R_m \equiv \frac{1}{2}(R_m^+(\mu_m) + R_m^-(\mu_m)), \quad (69)$$

we find well outside the cores of the constituents

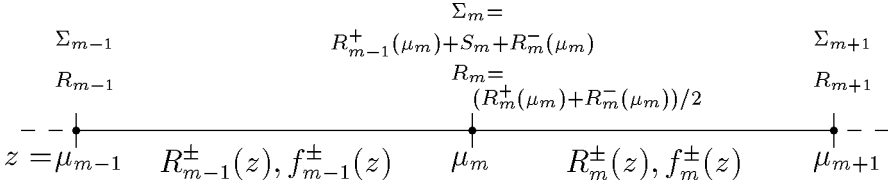
$$H_m \rightarrow \begin{pmatrix} \mathbb{1}_k & 0 \\ 2\pi R_m^+(\mu_{m+1}) & 0 \end{pmatrix} f_m^+(\mu_{m+1})(4\pi R_m)^{-1} \begin{pmatrix} 2\pi R_m^-(\mu_m) & \mathbb{1}_k \\ 0 & 0 \end{pmatrix}. \quad (70)$$

The sparse nature of the matrices involved will be of considerable help to simplify the limiting behavior of the Green's function. A crucial ingredient is the combination

$$\begin{pmatrix} 2\pi R_m^-(\mu_m) & \mathbb{1}_k \\ 0 & 0 \end{pmatrix} \begin{pmatrix} \mathbb{1}_k & 0 \\ 2\pi S_m & \mathbb{1}_k \end{pmatrix} \begin{pmatrix} \mathbb{1}_k & 0 \\ 2\pi R_{m-1}^+(\mu_m) & 0 \end{pmatrix} = \begin{pmatrix} 2\pi \Sigma_m & 0 \\ 0 & 0 \end{pmatrix},$$

$$\Sigma_m \equiv R_{m-1}^+(\mu_m) + R_m^-(\mu_m) + S_m, \quad (71)$$

for clarity summarizing the various ingredients in the following picture



This leads to the following far-field approximation for \mathcal{F}_{μ_m} (cf. Eq. (36)),

$$\mathcal{F}_{\mu_m} \rightarrow \hat{g}^\dagger(1) \begin{pmatrix} \mathbb{1}_k & 0 \\ 2\pi(R_{m+n-1}^+(\mu_{m+n}) + S_{m+n}) & 0 \end{pmatrix} \mathcal{G}_m \begin{pmatrix} 2\pi R_m^-(\mu_m) & \mathbb{1}_k \\ 0 & 0 \end{pmatrix} \quad (72)$$

where $\mathcal{G}_m \equiv \mathcal{G}_{m+n,m}$ and

$$\begin{aligned} \mathcal{G}_{m',m} &\equiv f_{m'-1}^+(\mu_{m'}) (2R_{m'-1})^{-1} \Sigma_{m'-1} f_{m'-2}^+(\mu_{m'-1}) (2R_{m'-2})^{-1} \\ &\times \Sigma_{m'-2} \cdots f_{m+1}^+(\mu_{m+2}) (2R_{m+1})^{-1} \Sigma_{m+1} f_m^+(\mu_{m+1}) (4\pi R_m)^{-1}. \end{aligned} \quad (73)$$

One might have expected a factor $2\pi \Sigma_m$ on the right, but this is contained in the remaining terms of Eq. (72). For example $\text{Tr}_k(\mathcal{F}_{\mu_m}) = \text{Tr}_k(\hat{g}^\dagger(1) \mathcal{G}_m (2\pi \Sigma_m))$.

As we have seen in Eqs. (37) and (39), the gauge field only requires us to know the Green's function at the impurities. Without loss of generality we may assume $\mu_{m'} > \mu_m$ and take $z_0 = \mu_m + 0$, such that (see Eqs. (23), (32), (35))

$$f_x(\mu_{m'}, \mu_m) = -4\pi^2 (\mathbb{1}_k, 0) \cdot W(\mu_{m'}, \mu_m + 0) (\mathbb{1}_{2k} - \mathcal{F}_{\mu_m})^{-1} \begin{pmatrix} 0 \\ \mathbb{1}_k \end{pmatrix}. \quad (74)$$

The matrix $(\mathbb{1}_{2k} - \mathcal{F}_{\mu_m})$ has a 2×2 block structure, and one can verify that in general

$$\begin{pmatrix} a & b \\ c & d \end{pmatrix}^{-1} = \begin{pmatrix} (a - bd^{-1}c)^{-1} & (c - db^{-1}a)^{-1} \\ (b - ac^{-1}d)^{-1} & (d - ca^{-1}b)^{-1} \end{pmatrix}. \quad (75)$$

Identifying the blocks, in the high temperature limit we find

$$\begin{aligned} a &\equiv (\mathbb{1}_{2k} - \mathcal{F}_{\mu_m})_{11} \rightarrow \mathbb{1}_k - 2\pi \hat{g}^\dagger(1) \mathcal{G}_m R_m^-(\mu_m), \\ b &\equiv (\mathbb{1}_{2k} - \mathcal{F}_{\mu_m})_{12} \rightarrow -\hat{g}^\dagger(1) \mathcal{G}_m, \\ c &\equiv (\mathbb{1}_{2k} - \mathcal{F}_{\mu_m})_{21} \rightarrow -4\pi^2 (R_{m-1}^+(\mu_m) + S_m) \hat{g}^\dagger(1) \mathcal{G}_m R_m^-(\mu_m), \\ d &\equiv (\mathbb{1}_{2k} - \mathcal{F}_{\mu_m})_{22} \rightarrow \mathbb{1}_k - 2\pi (R_{m-1}^+(\mu_m) + S_m) \hat{g}^\dagger(1) \mathcal{G}_m, \end{aligned} \quad (76)$$

where we used that $R_{m+n-1}^\pm(\mu_{m+n}) + S_{m+n} = \hat{g}(1)(R_{m-1}^\pm(\mu_m) + S_m)\hat{g}^\dagger(1)$, cf. Eqs. (34), (36). Evaluating the Green's function at the *same* impurities, $\mu_{m'} = \mu_m$, is simplified by the fact that $W(\mu_m, \mu_m) = \mathbb{1}_{2k}$. This gives the following remarkably simple result in the far-field limit,

$$f_x(\mu_m, \mu_m) = -4\pi^2(\mathbb{1}_{2k} - \mathcal{F}_{\mu_m})_{12}^{-1} \rightarrow 4\pi^2(2\pi\Sigma_m - \mathcal{G}_m^{-1}\hat{g}(1))^{-1} \rightarrow 2\pi(\Sigma_m)^{-1}. \quad (77)$$

For the Green's function evaluated at *different* impurities, $\mu_m \neq \mu_{m'}$, we need to determine $W(\mu_{m'} - 0, \mu_m + 0)$, for which we can follow the same method as for \mathcal{F}_{μ_m}

$$W(\mu_{m'} - 0, \mu_m + 0) = \begin{pmatrix} \mathbb{1}_k & 0 \\ 2\pi R_{m'-1}^+(\mu_{m'}) & 0 \end{pmatrix} \mathcal{G}_{m',m} \begin{pmatrix} 2\pi R_m^-(\mu_m) & \mathbb{1}_k \\ 0 & 0 \end{pmatrix}, \quad (78)$$

with $\mathcal{G}_{m',m}$ as defined in Eq. (73). This leads to

$$\begin{aligned} f_x(\mu_{m'}, \mu_m) &\rightarrow -4\pi^2 \mathcal{G}_{m',m} ((\mathbb{1}_{2k} - \mathcal{F}_{\mu_m})_{22}^{-1} + 2\pi R_m^-(\mu_m)(\mathbb{1}_{2k} - \mathcal{F}_{\mu_m})_{12}^{-1}) \\ &\rightarrow \mathcal{G}_{m',m} \mathcal{G}_m^{-1} \hat{g}(1) f_x(\mu_m, \mu_m), \end{aligned} \quad (79)$$

which is exponentially suppressed since $\mathcal{G}_{m',m}$ grows as $\exp(2\pi|\vec{x}|(\mu_{m'} - \mu_m))$. This cannot compensate for the decay of \mathcal{G}_m^{-1} , provided all μ_m are unequal, i.e., all constituents have a non-zero mass. Massless constituents have a so-called non-Abelian cloud [12], which has no Abelian far-field limit.

4.2. Total action

To determine ψ in the expression for the action density, Eqs. (46), (49), we need to compute $\det(\mathbb{1}_{2k} - \mathcal{F}_{\mu_m})$. Using Eq. (76) we find

$$\begin{aligned} \det(\mathbb{1}_{2k} - \mathcal{F}_{\mu_m}) &= \det \begin{pmatrix} a & b \\ c & d \end{pmatrix} = \det \begin{pmatrix} 0 & b \\ c - ab^{-1}d & d \end{pmatrix} = \det(b) \det(ab^{-1}d - c) \\ &\rightarrow \det(\hat{g}^\dagger(1)\mathcal{G}_m) \det(\mathcal{G}_m^{-1}\hat{g}(1) - 2\pi\Sigma_m) \rightarrow \det(-2\pi\hat{g}^\dagger(1)\mathcal{G}_m\Sigma_m), \end{aligned} \quad (80)$$

such that

$$\psi \rightarrow \det(\pi\mathcal{G}_m\Sigma_m) = 2^{-k} \prod_{m=1}^n \{ \det(f_m^+(\mu_{m+1})) \det(\Sigma_m) / \det(2R_m) \}. \quad (81)$$

For $|\vec{x}| \rightarrow \infty$, $f_m^+(\mu_{m+1}) \rightarrow \exp(2\pi v_m |\vec{x}| \mathbb{1}_k)$ (see Eq. (65)) and $\frac{1}{2}\Sigma_m$, $R_m \rightarrow |\vec{x}| \mathbb{1}_k$, which implies that $\psi \rightarrow 2^{-k} \prod_{m=1}^n \det[\exp(2\pi v_m |\vec{x}| \mathbb{1}_k)] = 2^{-k} \exp(2\pi k |\vec{x}|)$ (recall that $\sum_{m=1}^n v_m = 1$). Therefore, the action is given by $S = -\frac{1}{2} \int d^4x \partial_\mu^2 \partial_\nu^2 \log \psi(x) = 8\pi^2 k$, as should be the case for a self-dual charge k solution.

4.3. Gauge field

Without the off-diagonal components of the Green's function contributing to the far-field region, the functions ϕ and ϕ_j in Eqs. (37), (39) can be further simplified to

$$\begin{aligned}\phi(x)^{-1} &\rightarrow 1 - \sum_m \hat{f}^{ab}(\mu_m, \mu_m) P_m \zeta_a \zeta_b^\dagger P_m, \\ \phi_j &\rightarrow \sum_m \hat{f}^{ab}(\mu_m, \mu_m) P_m \zeta_a \hat{\sigma}_j \zeta_b^\dagger P_m,\end{aligned}\quad (82)$$

and only the Abelian components of the gauge field survive. Particularly the case of $Sp(1)$ discussed in Section 2.3 is easy to deal with. Using Eqs. (23), (40), (42), (44), (77) we find

$$\begin{aligned}\phi^{-1}(x) &\rightarrow \sigma_0(1 - \text{Tr}_k[2\Sigma_2^{-1}S_2]) \equiv \sigma_0\phi_{\text{ff}}^{-1}(x), \\ \vec{\phi}(x) &\rightarrow \hat{\omega} \cdot \vec{\sigma} \text{Tr}_k[2\Sigma_2^{-1}\hat{g}(\mu_2)\vec{\rho}_2\hat{g}^\dagger(\mu_2)], \\ A_\mu(x) &\rightarrow \frac{i}{2}\hat{\omega} \cdot \vec{\tau}(1 - \text{Tr}_k[2\Sigma_2^{-1}S_2])^{-1}\bar{\eta}_{\mu\nu}^j\partial_\nu \text{Tr}_k[2\Sigma_2^{-1}\hat{g}(\mu_2)\rho_2^j\hat{g}^\dagger(\mu_2)],\end{aligned}\quad (83)$$

where we recall (see Eq. (71)) that $\Sigma_2 = (R_1^+(\mu_2) + R_2^-(\mu_2) + S_2)$. This is in perfect agreement with the earlier $k = 1$ results [1]. Note that the gauge rotation which relates $\hat{f}_x(z, z')$ to $f_x(z, z')$ also relates \hat{S}_m to S_m (see Eqs. (23), (24)) and therefore does not appear in the final expression for $\phi(x)$.

It is interesting to note that the dipole moment of the Abelian gauge field is particularly simple and does not require us to solve for $R_m^\pm(z)$, since $\lim_{|\vec{x}|\rightarrow\infty} \Sigma_2 = 2|\vec{x}|\mathbb{1}_k$ such that

$$\lim_{|\vec{x}|\rightarrow\infty} A_\mu(x) = \frac{i}{2}\hat{\omega} \cdot \vec{\tau} \bar{\eta}_{\mu\nu}^j \partial_\nu \frac{\text{Tr}_k(\rho_2^j)}{|\vec{x}|}.\quad (84)$$

Hence the dipole moment $\vec{p} \equiv \frac{1}{2}\text{Tr}_k(\vec{\rho}_2)$ only involves ζ_a , and we do except it allows for configurations with a vanishing dipole moment. For higher multipole moments, through $R_m^\pm(z)$, we need to deal with the full quadratic ADHM constraint, or equivalently with the Riccati and Nahm equations. Nevertheless, it is remarkable that in the high temperature limit the \vec{x} dependence is restricted to $R_1^+(\mu_2)$ and $R_2^-(\mu_2)$ only. We would like to prove that each of its eigenvalues vanish at an isolated point, as one way to identify the $2k$ constituent locations. We will defer the study of this interesting issue, and its generalization to $SU(n)$, to a future publication.

4.3.1. Axially symmetric case

The far-field approximation further simplifies when considering the axially symmetric solutions discussed in Section 3.2. We restrict ourselves here to $Sp(1)$. Since $\vec{R}(z; \vec{x})$ is piecewise constant, the Riccati equation is trivial to solve,

$$R_m^\pm(z) = R_m = \sqrt{(\vec{x}\mathbb{1}_k - \vec{e}Y_m) \cdot (\vec{x}\mathbb{1}_k - \vec{e}Y_m)}.\quad (85)$$

The square root involves a positive $k \times k$ matrix, and is well-defined. Due to the fact that $S_m = \hat{g}(\mu_m)\hat{S}_m\hat{g}^\dagger(\mu_m) = \hat{g}(\mu_m)\Delta\vec{y}_m \cdot \vec{\rho}_m/|\Delta y_m|\hat{g}^\dagger(\mu_m)$ (see Eqs. (24), (59)), the Abelian

component of the gauge field is of the simple form ($\vec{e} = \vec{\rho}_2/|\vec{\rho}_2|$, see Section (2.3))

$$A_\mu^{\text{abel}}(x) = -\frac{i}{2}\hat{\omega} \cdot \vec{e}_j \bar{\eta}_{\mu\nu}^j \partial_\nu \log \phi(x). \quad (86)$$

In the far field limit $\phi(x) \rightarrow \phi_{\text{ff}}(x)$ (see Eq. (83)). Since S_2 has rank 1, the matrix $M \equiv 2\Sigma_2^{-1}S_2$ has only one non-vanishing column with respect to a suitably chosen basis, which implies that $1 - \text{Tr}_k(M) = \det(\mathbb{1}_k - M)$. This allows us to write in the far-field region

$$\phi_{\text{ff}}(x) = \frac{\det(R_1 + R_2 + S_2)}{\det(R_1 + R_2 - S_2)}, \quad (87)$$

from which we immediately read off the result [1] for $k = 1$, in which case it is easy to show that $\phi_{\text{ff}}(x) = (r_2 + \vec{e} \cdot \vec{r}_2)/(r_1 + \vec{e} \cdot \vec{r}_1)$, revealing $A_\mu(x)$ to be a linear superposition of two oppositely charged self-dual Dirac monopoles. We would like $\phi_{\text{ff}}(x)$ to similarly factorize for $k > 1$ in $2k$ Dirac monopoles, but since R_1 , R_2 and S_2 in general do not commute, some care is required in demonstrating the factorization. We will rely on the fact that $(R_m - \vec{e} \cdot \vec{R}_m)(R_m + \vec{e} \cdot \vec{R}_m) = (R_m + \vec{e} \cdot \vec{R}_m)(R_m - \vec{e} \cdot \vec{R}_m) = R_m^2 - (\vec{e} \cdot \vec{R}_m)^2 = (\vec{x} \times \vec{e})^2 \mathbb{1}_k$ and hence independent of m . Since by definition $\Delta y_2 > 0$ (see Section 3.2), one finds that

$$\phi_{\text{ff}}(x) = \frac{\det((R_1 - \vec{e} \cdot \vec{R}_1) + (R_2 + \vec{e} \cdot \vec{R}_2))}{\det((R_2 - \vec{e} \cdot \vec{R}_2) + (R_1 + \vec{e} \cdot \vec{R}_1))}. \quad (88)$$

This can now be reorganized according to

$$\begin{aligned} \phi_{\text{ff}}(x) &= \frac{\det(((R_1 - \vec{e} \cdot \vec{R}_1) + (R_2 + \vec{e} \cdot \vec{R}_2))(R_1 + \vec{e} \cdot \vec{R}_1)) \det(R_2 + \vec{e} \cdot \vec{R}_2)}{\det((R_2 + \vec{e} \cdot \vec{R}_2)((R_2 - \vec{e} \cdot \vec{R}_2) + (R_1 + \vec{e} \cdot \vec{R}_1))) \det(R_1 + \vec{e} \cdot \vec{R}_1)} \\ &= \frac{\det(R_2 + \vec{e} \cdot \vec{R}_2)}{\det(R_1 + \vec{e} \cdot \vec{R}_1)}, \end{aligned} \quad (89)$$

after which we can separately diagonalize \vec{R}_1 and \vec{R}_2 to find

$$\phi_{\text{ff}}(x) = \prod_i \frac{r_2^{(i)} + \vec{e} \cdot \vec{r}_2^{(i)}}{r_1^{(i)} + \vec{e} \cdot \vec{r}_1^{(i)}} = \prod_i \frac{r_1^{(i)} + r_2^{(i)} + |y_1^{(i)} - y_2^{(i)}|}{r_1^{(i)} + r_2^{(i)} - |y_1^{(i)} - y_2^{(i)}|}, \quad (90)$$

where $y_m^{(i)} \vec{e}$ give the locations of the constituent monopoles, with $y_m^{(i)}$ the eigenvalues of Y_m and $\vec{r}_m^{(i)} = \vec{x} - y_m^{(i)} \vec{e}$ (the index m distinguishing their charge). The second expression for the factorized version of $\phi_{\text{ff}}(x)$ uses the fact that the constituent locations can be ordered according to

$$y_1^{(1)} < y_2^{(1)} < y_1^{(2)} < y_2^{(2)} < \dots < y_1^{(k)} < y_2^{(k)}. \quad (91)$$

It should be noted that this prevents the constituents to pass each other while varying the parameters for the axially symmetric configuration, see also Fig. 3 and the discussion in Section 3.2. We need to go beyond this simple axially symmetric configuration to allow for the constituents to rearrange themselves more freely.

5. Discussion

We have presented the general formalism for finding exact instanton solutions at finite temperature (calorons) with any non-trivial holonomy and topological charge. In an infinite volume holonomy and charge are fixed. The solution is described by $4kn$ parameters of which $3kn$ give the spatial locations of the kn constituent monopoles. The remaining parameters are given by k time locations and $(n-1)k$ phases associated to gauge rotations in the subgroup that leaves the holonomy unchanged. Of these, $n-1$ can be considered as global gauge rotations. The dimension of the moduli space, i.e., the number of gauge invariant parameters, is therefore equal to $4kn - (n-1)$. Our subset of axially symmetric solutions has $2nk + 4$ parameters of which there are $n-1$ global gauge rotations, or $2nk - n + 5$ gauge invariant parameters.

Explicit solutions were found for the case of axial symmetry, an important limitation being the difficulty of solving the Nahm equation, or equivalently the quadratic ADHM constraint. We certainly expect more progress can be made on this in the near future. Nevertheless, we already found a rich structure that bodes well for being able to consider the constituent monopoles as independent objects. This is surprisingly subtle, as we have illustrated by the fact that an approximate superposition of charge 1 calorons tends to give rise to a *visible* Dirac string. This is also related to the difficulty of finding approximate multi-monopole solutions, which can be obtained from the caloron solutions by sending a subset of the constituent monopoles to infinity, as has been well studied in the charge 1 case [1,13].

An important tool has been our study of the far-field limit, describing the Abelian gauge field far removed from any of the constituent monopoles. This allows for a description of the long distance properties in terms of (self-dual) Dirac monopoles. Much could be extracted concerning its properties without the need to explicitly solve the Nahm equation. We conjecture in general to be able to identify the Dirac monopole location, but some work remains to be done here.

It may seem that all these results are somewhat academic since until recently none of these constituent monopoles were found in dynamical lattice configurations. First of all one would be tempted to search for them at high temperature, but it should be noted that above the deconfining phase transition the average Polyakov loop takes on trivial values, associated to the center of the gauge group, which is not the environment in which a caloron will reveal its constituents. This would give the well-known Harrington–Shepard solution constructed long ago [14]. With our present understanding this solution can be seen as having $n-1$ massless constituents which cannot be localized. Only when sending all these to infinity one is left with a monopole [15]. Furthermore, at high temperature classical configurations will be heavily suppressed due to their Boltzmann weight. Rather, the hope is that the constituent monopoles play an important role *below* the deconfining temperature, where the average of the Polyakov loop is non-trivial, and tends to favor *equal* mass constituents. This is why in this paper our examples were for that case, see Figs. 2, 4, 5 and the discussion in Section 3.2. Nevertheless, the formalism developed here gives results for any choice of the holonomy, and a sample of unequal mass constituents is given in Fig. 6. In general the constituent monopoles can be characterized by their magnetic

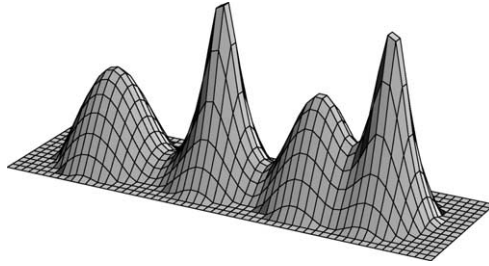


Fig. 6. The logarithm of the action density (cutoff for $\log(S)$ below -3) for an $SU(2)$ charge 2 caloron with one type of constituent three times more massive than the other ($\mu_2 = 1/8$, $\alpha_a^j = \xi_0^a = 0$, $\rho_j = 2$, $\xi = 3.5$).

(= electric) charge. For $SU(n)$ there are n different types of Abelian charges involved [1], and all k constituents of a given type have the same mass.

We will discuss briefly the lattice evidence for the presence of constituent monopoles that has accumulated the last few years. A first numerical study using cooling was performed with twisted boundary conditions, which implies non-trivial holonomy [16]. Good agreement was found with the infinite volume charge 1 analytic results, in particular so for the fermion zero-modes [17,18] which are more localized than the action density. A charge 2 solution was also found, shown in Fig. 8 of Ref. [16]. Fermion zero-modes played an intricate role in an extensive numerical study of Nahm dualities on the torus [19].

As suggested in Ref. [1] one may also enforce non-trivial holonomy on the lattice by putting at the spatial boundary of the box all links in the time direction to the same constant value U_0 , such that $U_0^{N_t} = \mathcal{P}_\infty$ (N_t the number of lattice sites in the time direction). This has been implemented in $SU(2)$ lattice Monte Carlo studies as well, where \mathcal{P}_∞ was set to the average value of the Polyakov loop, appropriate for the temperature at which the simulations were performed [20,21]. Cooling was applied to find calorons, including those at higher charge. Apart from the configurations that in the continuum would be exactly self-dual, the lattice allows one to also consider configurations in which both self-dual and anti-selfdual lumps appear. This revealed constituent monopoles that seem not directly associated to calorons, called $D\bar{D}$ (as opposed to DD). Both objects in such a $D\bar{D}$ configuration have fractional topological charged, but opposite in sign. Perhaps these arise when two near constituent monopoles, one belonging to a caloron, the other to an anti-caloron, “annihilate”. Our analytic methods cannot directly address this situation due to the lack of self-duality. The same holds for configurations that seem to only carry magnetic fields, which were already seen long ago [22].

One point of criticism that applies to both methods is that the choice of boundary conditions may force the “dissociation” of instantons into constituent monopoles, particularly since volumes cannot yet be chosen so large that many instantons are contained within a given configuration. A recent study [23] has done away with the fixed boundary conditions that enforce the non-trivial holonomy. Nevertheless, still one finds in many cases that calorons “dissociate” into constituent monopoles below the deconfinement transition temperature. A particularly useful tool has turned out to be the fermionic (near) zero-modes to detect the monopole constituents when they are too close together to reveal themselves from the action density [23]. This relies on the observation that the zero-mode is localized

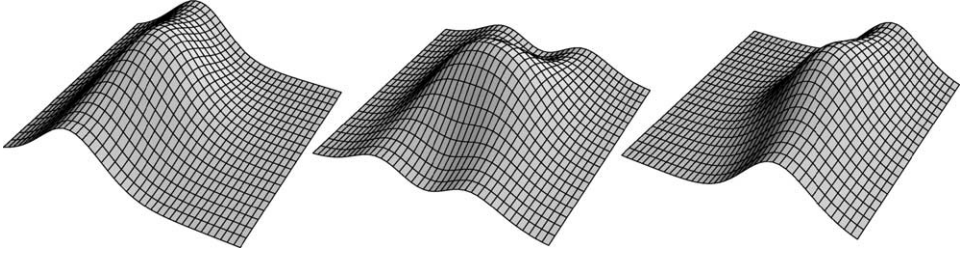


Fig. 7. Fermion zero-mode densities as a function of t and z for a charge 1 caloron ($\mu_2 = \frac{1}{4}$ and $\rho = \frac{1}{2}$) with periodic (right) and anti-periodic (left) boundary conditions, compared to the action density (middle) (see also Fig. 5 in Ref. [26]). Based on Ref. [25]; produced with Ref. [27]).

on *only* one of the constituent monopoles, determined by the boundary conditions imposed on the fermions in the time direction [17,18]. For $SU(2)$ this is particularly simple, with periodic and anti-periodic boundary conditions of the fermions making the zero-mode switch from one constituent to the other, as is illustrated for a close pair of constituents in Fig. 7. In addition one may use the Polyakov loop for diagnostic purposes [20,21,23], for $SU(2)$ taking the values $\mathbb{1}_2$ and $-\mathbb{1}_2$ near the respective constituent locations (at these points the gauge symmetry is restored, providing an alternative definition for the center of a constituent monopole).

Fermion eigenfunctions with eigenvalues near zero have also been used as an alternative to cooling, to filter out the high frequency modes and identify topological lumps. For a recent lattice study, including some discussion of calorons with non-trivial holonomy, see Ref. [24] and references therein. Using the near zero-modes as a filter, constituent monopoles have even been identified recently for $SU(3)$ well below the deconfining temperature [25], resembling Fig. 7 (see also Fig. 14 of Ref. [24]).

For the exact axially symmetric multi-caloron solutions constructed in this paper the k associated fermion zero-modes (for charge k) will be derived in the near future. We anticipate that one can choose a basis where each is localized on one of the constituent monopoles, the type of which is determined by the choice of fermionic boundary conditions in the time direction. Analyzing these zero-modes is particularly interesting in the light of some puzzles that were presented in a recent study [28] of the normalizable fermion zero-modes in the background of a collection of so-called bipoles, i.e., pairs of oppositely charged (but self-dual) Dirac monopoles, which are of interest in a wider context as well. This will be one of the many topics we have access to with our analytic tools. But ultimately our main aim is to develop a reliable method to describe the long distance features of non-Abelian gauge theories in terms of monopole constituents to understand both confinement and chiral symmetry breaking. The results of this paper, and in particular the recent lattice results, provide some encouragement in this direction.

Acknowledgements

We thank Conor Houghton for initial collaboration on the monopole aspects of this work and him as well as Chris Ford for extensive discussions. P.v.B. also thanks Michael

Müller-Preussker and Christof Gattringer for discussions concerning calorons with non-trivial holonomy on the lattice. Furthermore he is grateful to Leo Stodolsky and Valya Zakharov for hospitality at the MPI in Munich and to Poul Damgaard, Urs Heller and Jac Verbaarschot for inviting him to the ECT* workshop “Non-perturbative Aspects of QCD” in Trento. He thanks both institutions for their support, while some of the work presented in this paper was performed. F.B. likes to thank the organizers of the “Channel Meeting on Theoretical Particle Physics” for a well organized and stimulating meeting as well as Dimitri Diakonov, Gerald Dunne, Alexander Gorsky and Peter Orland for discussions. The research of F.B. is supported by FOM.

References

- [1] T.C. Kraan, P. van Baal, Phys. Lett. B 428 (1998) 268, hep-th/9802049;
T.C. Kraan, P. van Baal, Nucl. Phys. B 533 (1998) 627, hep-th/9805168.
- [2] T.C. Kraan, P. van Baal, Phys. Lett. B 435 (1998) 389, hep-th/9806034.
- [3] M.F. Atiyah, N.J. Hitchin, V.G. Drinfeld, Yu.I. Manin, Phys. Lett. A 65 (1978) 185;
M.F. Atiyah, Geometry of Yang–Mills fields, Fermi lectures, Scuola Normale Superiore, Pisa, 1979.
- [4] W. Nahm, Self-dual monopoles and calorons, in: G. Denardo (Ed.), in: Lecture Notes in Physics, Vol. 201, 1984, p. 189.
- [5] K. Lee, P. Yi, Phys. Rev. D 56 (1997) 3711, hep-th/9702107;
K. Lee, Phys. Lett. B 426 (1998) 323, hep-th/9802012;
K. Lee, C. Lu, Phys. Rev. D 58 (1998) 025011, hep-th/9802108.
- [6] W. Nahm, Phys. Lett. B 90 (1980) 413.
- [7] G. 't Hooft, Nucl. Phys. B 190 (1981) 455;
G. 't Hooft, Phys. Scr. 25 (1982) 133.
- [8] E.F. Corrigan, D.B. Fairlie, S. Templeton, P. Goddard, Nucl. Phys. B 140 (1978) 31.
- [9] H. Osborn, Nucl. Phys. B 159 (1979) 497.
- [10] M. García Pérez, T.G. Kovács, P. van Baal, Phys. Lett. B 472 (2000) 295, hep-ph/9911485.
- [11] P. van Baal, in: V. Mitrushkin, G. Schierholz (Eds.), Lattice Fermions and Structure of the Vacuum, Kluwer Academic, Dordrecht, 2000, p. 269, hep-th/9912035.
- [12] K. Lee, E.J. Weinberg, P. Yi, Phys. Lett. B 376 (1996) 97, hep-th/9601097;
K. Lee, E.J. Weinberg, P. Yi, Phys. Rev. D 54 (1996) 6351, hep-th/9605229;
E.J. Weinberg, Massive and massless monopoles and duality, hep-th/9908095.
- [13] T.C. Kraan, Commun. Math. Phys. 212 (2000) 503, hep-th/9811179.
- [14] B.J. Harrington, H.K. Shepard, Phys. Rev. D 17 (1978) 2122;
B.J. Harrington, H.K. Shepard, Phys. Rev. D 18 (1978) 2990.
- [15] P. Rossi, Nucl. Phys. B 149 (1979) 170.
- [16] M. García Pérez, A. González-Arroyo, A. Montero, P. van Baal, J. High Energy Phys. 06 (1999) 001, hep-lat/9903022.
- [17] M. García Pérez, A. González-Arroyo, C. Pena, P. van Baal, Phys. Rev. D 60 (1999) 031901, hep-th/9905016.
- [18] M.N. Chernodub, T.C. Kraan, P. van Baal, Nucl. Phys. B (Proc. Suppl.) 83–84 (2000) 556, hep-lat/9907001.
- [19] M. García Pérez, A. González-Arroyo, C. Pena, P. van Baal, Nucl. Phys. B 564 (1999) 159, hep-th/9905138.
- [20] E.-M. Ilgenfritz, M. Müller-Preussker, A.I. Veselov, in: V. Mitrushkin, G. Schierholz (Eds.), Lattice Fermions and Structure of the Vacuum, Kluwer Academic, Dordrecht, 2000, p. 345, hep-lat/0003025.
- [21] E.-M. Ilgenfritz, B.V. Martemyanov, M. Müller-Preussker, A.I. Veselov, Nucl. Phys. B (Proc. Suppl.) 94 (2001) 407, hep-lat/0011051;
E.-M. Ilgenfritz, B.V. Martemyanov, M. Müller-Preussker, A.I. Veselov, Nucl. Phys. B (Proc. Suppl.) 106 (2002) 589, hep-lat/0110212.
- [22] M.L. Laursen, G. Schierholz, Z. Phys. C 38 (1988) 501.

- [23] E.-M. Ilgenfritz, B.V. Martemyanov, M. Müller-Preussker, S. Shcheredin, A.I. Veselov, hep-lat/0206004.
- [24] C. Gattringer, M. Göckeler, P.E.L. Rakow, S. Schaefer, A. Schäfer, Nucl. Phys. B 618 (2001) 205, hep-lat/0105023.
- [25] Christof Gattringer, private communications. The zero-mode densities for the case of Fig. 7 were produced for the purpose of illustrating the behavior observed by C. Gattringer and co-workers in $SU(3)$ lattice gauge theory.
- [26] T.C. Kraan, P. van Baal, Nucl. Phys. B (Proc. Suppl.) 73 (1999) 554, hep-lat/9808015.
- [27] <http://www.lorentz.leidenuniv.nl/vanbaal/Caloron.html>.
- [28] P. van Baal, Chiral zero-modes for Abelian BPS dipoles, in: J. Greensite, S. Olejnik (Eds.), Confinement, Topology, and other Non-Perturbative Aspects of QCD, Kluwer Academic, in press, hep-th/0202182.